A13

KEK Preprint 97-210
KOBE HEP 97-03
NGTHEP 97-3
OULNS 97-02
November 1997
H

Precise measurement of the $e^+e^- \to \mu^+\mu^-$ reaction at $\sqrt{s} = 57.77$ GeV

VENUS Collaboration

The reaction $e^+e^- \to \mu^+\mu^-$ has been measured at $\sqrt{s}$ = 57.77 GeV, based on 289.6 ± 2.6 pb^{-1} data collected with the VENUS detector at TRISTAN. The production cross section is measured in bins of the production angle within an angular acceptance of $|\cos\theta| \leq 0.75$, according to a model-independent definition. The result is consistent with the prediction of the standard electroweak theory. Although a trend in measurements at lower energies that the total cross section tends to be smaller than the prediction remains, the discrepancy is not significant. The model-independent result is converted to the differential cross section in the effective-Born scheme by unfolding photon-radiation effects. This result can be extrapolated to quantities for the full solid angle as $\sigma_{\rm TOT}^{\rm EB} = 30.05 \pm 0.59$ pb and $A_{\rm FB}^{\rm EB} = -0.350 \pm 0.017$, by imposing an ordinary assumption on the production-angle dependence. The converted results are used to set constraints on extensions of the standard theory. S-matrix parametrization, and possible contributions from contact interactions and heavy neutral-scalar exchanges are examined.

Submitted to Physical Review D.

** From April 1, 1997, **High Energy Accelerator Research Organization (KEK)** was newly established. The new organization is restructured of three reseach institutes, National Laboratory for High Energy Physics (KEK), Institues of Nuclear Study (INS), Univ. of Tokyo and Meson Science Laboratory, Faculty of Science, Univ. of Tokyo.*

High Energy Accelerator Research Organization (KEK), 1997

KEK Reports are available from:

Information Resources Division
High Energy Accelerator Research Organization (KEK)
1-1 Oho, Tsukuba-shi
Ibaraki-ken, 305
JAPAN

Phone: 0298-64-5137
Fax: 0298-64-4604
Cable: KEK OHO
E-mail: Library@kekvax.kek.jp (Internet Address)
Internet: http://www.kek.jp

Precise measurement of the $e^+e^- \to \mu^+\mu^-$ reaction at $\sqrt{s} = 57.77$ GeV

M. Miura,[3,*] S. Odaka,[2,†] T. Arima,[3,‡] K. Tobimatsu,[20] K. Ogawa,[2,§] J. Shirai,[2,**] T. Tsuboyama,[2] K. Abe,[1] K. Amako,[2] Y. Arai,[2] Y. Asano,[3] M. Chiba,[4] Y. Chiba,[5] M. Daigo,[6] M. Fukawa,[2,††] Y. Fukushima,[2] J. Haba,[2] H. Hamasaki,[3] Y. Hemmi,[7] M. Higuchi,[8] T. Hirose,[4] Y. Homma,[9] N. Ishihara,[2] Y. Iwata,[10] J. Kanzaki,[2] R. Kikuchi,[7] T. Kondo,[2] T. T. Korhonen,[2,11,‡‡] H. Kurashige,[7] E. K. Matsuda,[12] T. Matsui,[2] K. Miyake,[7] S. Mori,[3] Y. Nagashima,[13] Y. Nakagawa,[14,§§] T. Nakamura,[12,***] I. Nakano,[15] T. Ohama,[2] T. Ohsugi,[10] H. Ohyama,[16] K. Okabe,[15] A. Okamoto,[7] A. Ono,[17] J. Pennanen,[2,11] H. Sakamoto,[7] M. Sakuda,[2] M. Sato,[8] N. Sato,[2] M. Shioden,[18] T. Sumiyoshi,[2] Y. Takada,[3] F. Takasaki,[2] M. Takita,[13] N. Tamura,[19] D. Tatsumi,[13,†††] S. Uehara,[2] Y. Unno,[2] T. Watanabe,[21] Y. Watase,[2] F. Yabuki,[4] Y. Yamada,[2] T. Yamagata,[14] Y. Yonezawa,[22] H. Yoshida,[23] and K. Yusa[3,‡‡‡]

(VENUS Collaboration)

[1] *Department of Physics, Tohoku University, Sendai 980, Japan*

[2] *High Energy Accelerator Research Organization (KEK), Tsukuba 305, Japan*

[3] *Institute of Applied Physics, University of Tsukuba, Tsukuba 305, Japan*

[4] *Department of Physics, Tokyo Metropolitan University, Hachioji 192-03, Japan*

[5] *Yasuda Women's Junior College, Hiroshima 731-01, Japan*

[6] *Faculty of Economics, Toyama University, Toyama 930, Japan*

[7] *Department of Physics, Kyoto University, Kyoto 606, Japan*

[8] *Department of Applied Physics, Tohoku-Gakuin University, Tagajo 985, Japan*

[9] *Faculty of Engineering, Kobe University, Kobe 657, Japan*

[10] *Department of Physics, Hiroshima University, Higashi-Hiroshima 724, Japan*

[11] *Research Institute for High Energy Physics, Helsinki University, SF-00170 Helsinki, Finland*

[12] *Faculty of Engineering, Miyazaki University, Miyazaki 889-01, Japan*

[13] *Department of Physics, Osaka University, Toyonaka 560, Japan*

[14] *International Christian University, Mitaka 181, Japan*

[15] *Department of Physics, Okayama University, Okayama 700, Japan*

[16] *Hiroshima National College of Maritime Technology, Higashino 725-02, Japan*

[17] *Faculty of Cross-Cultural Studies, Kobe University, Kobe 657, Japan*

[18] *Ibaraki College of Technology, Katsuta 312, Japan*

[19] *Department of Physics, Niigata University, Niigata 950-21, Japan*

[20] *Center for Information Science, Kogakuin University, Tokyo 163-91, Japan*

[21] *Department of Physics, Kogakuin University, Hachioji 192, Japan*

[22] *Tsukuba College of Technology, Tsukuba 305, Japan*

[23] *Naruto University of Education, Naruto 772, Japan*

(October 28, 1997)

Abstract

The reaction $e^+e^- \to \mu^+\mu^-$ has been measured at $\sqrt{s} = 57.77$ GeV, based on 289.6 ± 2.6 pb^{-1} data collected with the VENUS detector at TRISTAN. The production cross section is measured in bins of the production angle within an angular acceptance of $|\cos\theta| \leq 0.75$, according to a model-independent definition. The result is consistent with the prediction of the standard electroweak theory. Although a trend in measurements at lower energies that the total cross section tends to be smaller than the prediction remains, the discrepancy is not significant. The model-independent result is converted to the differential cross section in the effective-Born scheme by unfolding photon-radiation effects. This result can be extrapolated to quantities for the full solid angle as $\sigma_{\rm TOT}^{\rm EB} = 30.05 \pm 0.59$ pb and $A_{\rm FB}^{\rm EB} = -0.350 \pm 0.017$, by imposing an ordinary assumption on the production-angle dependence. The converted results are used to set constraints on extensions of the standard theory. S-matrix parametrization, and possible contributions from contact interactions and heavy neutral-scalar exchanges are examined.

PACS numbers: 13.10.+q, 14.60.Ef, 12.60.-i

Typeset using REVTEX

*Present address: Institute for Cosmic Ray Research, University of Tokyo, Tanashi 188, Japan.

†Corresponding author. Electronic address: shigeru.odaka@kek.jp.

‡Present address: Faculty of Engineering, Kyushu University, Fukuoka 812, Japan.

§Deceased.

**Present address: Department of Physics, Tohoku University, Sendai 980, Japan.

††Present address: Naruto University of Education, Naruto 772, Japan.

‡‡Present address: Accelerator Laboratory, KEK, Tsukuba 305, Japan.

§§Present address: Faculty of Science, Ehime University, Matsuyama 790, Japan.

***Deceased.

†††Present address: Institute for Cosmic Ray Research, University of Tokyo, Tanashi 188, Japan.

‡‡‡Present address: Department of Physics, The Cancer Institute, Kami-Ikebukuro 170, Japan.

I. INTRODUCTION

The muon pair production in electron-positron annihilation,

$$e^+e^- \to \mu^+\mu^-, \tag{1}$$

is one of the simplest reactions of the neutral current. This reaction is simpler than Bhabha scattering, because of the absence of t-channel interactions. The simple final state provides less ambiguous information on the production process, compared to analogous quark-pair productions. These are the reasons why the electroweak effect in e^+e^- annihilation was first observed in this reaction [1]. Since then, reaction (1) has been extensively studied by many experiments at high-energy e^+e^- colliders [2–7], and has played an important role in studies of the neutral-current properties.

The standard electroweak theory [8] has been very successful in all fields of the elementary particle physics. Within the framework of this theory, reaction (1) is described with s-channel exchanges of the photon and the Z^0 boson. The validity of this picture has been precisely tested by experiments at the LEP and SLC colliders on the Z^0 resonance, $\sqrt{s} \approx 90$ GeV [6], as well as those at the PEP and PETRA colliders below the resonance, $\sqrt{s} = 12 - 46$ GeV [2,3]. The Z^0 exchange dominates the reaction in the former, while the photon exchange is dominant in the latter. Recently, measurements above the Z^0 resonance are also becoming available [7]. No significant deviation from the standard theory has been reported from these experiments.

However, by looking at the results closely, we can find a systematic deficit of a few percent with respect to the standard theory, in the measured total cross section near the maximum energy of the PETRA experiments, $\sqrt{s} = 35 - 46$ GeV [9,10]. Whereas, the forward-backward (FB) asymmetry, another important measure used to characterize this reaction, is in good agreement with the standard theory. This trend remained in early results from experiments at the TRISTAN collider, $\sqrt{s} = 50 - 64$ GeV [4,5], although the precision was limited due to poor statistics.

The deficit in the total cross section can be explained by the existence of a new heavy neutral boson having a substantial vector coupling to leptons [10]. The exchange of such a boson results in a destructive interference with the photon exchange, thus suppressing the cross section. On the other hand, the FB asymmetry is not affected if the axial-vector coupling is small. The effects may be invisible in the Z^0 resonance region if the mixing with Z^0 is small. Such a boson is, of course, out of the scope of the standard theory. Therefore, if the deficit is proved to be real, it will be strong evidence for new physics beyond the standard theory.

Experiments at the TRISTAN collider of KEK have accumulated high-statistics e^+e^--collision data at a center-of-mass energy ($\sqrt{s}$) of 57.77 GeV, during runs from 1991 until the end of the experiments in May, 1995. These data are expected to be suitable for exploring this problem.

In this paper we present results from a measurement of reaction (1), using data accumulated with the VENUS detector at TRISTAN. The data used for the measurement correspond to an integrated luminosity of 290 pb^{-1}. These data provide us with about 4500 muon-pair events within an angular acceptance of $|\cos\theta| \leq 0.75$.

The layout of this paper is as follows: The relevant features of the VENUS detector and the event trigger are described in Section II. The determination of the integrated luminosity is also described there. The determination is based on the measurement of Bhabha scattering, described in our previous report [11]. The main subject in this section is to evaluate the error in the theoretical estimation of the corresponding cross section. Possible contributions from unexpected new interactions are taken into consideration.

The event selection is described in Section III. Corrections for the detection inefficiency and the background contamination are described in Section IV, emphasizing careful estimations of associated systematic errors. The corrections are estimated in bins of the production angle. The error correlation between the bins is treated in the form of an error (covariance) matrix. The corrections are applied to the measured number of events to obtain a model-independent cross section. In our energy region, the model dependence mainly concerns the radiative correction relevant to photon radiations [11]. The primary measurement result is presented in a form which includes the photon-radiation effects; namely, it is given for the reaction

$$e^+e^- \to \mu^+\mu^- + n\gamma \quad (n = 0, 1, ..., \infty) \tag{2}$$

with appropriate constraints on the muon pair in the final state.

Section V is dedicated to discussions on the underlying physics. The model-independent result is compared with theoretical predictions based on the standard theory, including the radiative correction. An explicit definition of the signal events allows us to make comparisons without any ambiguity. Comparisons are also carried out with theories including certain extensions from the standard theory, in order to examine the sensitivity to new phenomena. These comparisons are made after correcting the primary result for the effects of the photon radiation. This correction makes it easier to discuss underlying short-range interactions, though the result may suffer from a certain model-dependence. Finally, the conclusions are summarized in Section VI.

II. EXPERIMENT

A. The VENUS detector

The VENUS detector was a general-purpose magnetic spectrometer, equipped with a thin superconducting solenoid [12] producing a 0.75-Tesla axial magnetic field. It was placed at one of the four interaction points of the TRISTAN e^+e^- collider [13] of KEK. The detector was operated since the commissioning of TRISTAN in November, 1986, until the end of the experiment in May, 1995. There was an upgrade of both the detector and the accelerator in 1990. The present measurement is based on data accumulated after the upgrade.

A quadrant cross section of the upgraded VENUS detector is shown in Fig. 1. The vacuum pipe of the TRISTAN main ring penetrated the detector along its center axis. Bunched electron and positron beams, circulated in opposite directions through the pipe, provided collisions near the center of the detector. The spread of the interaction point was 1.0 cm along the beam direction in rms, with a transverse spread of about 300 μm horizontally and 20 μm vertically. The average offset of the interaction point was 5 mm

from the detector center along the beam direction and 0.3 mm in the transverse plane. The drift of the average position was within ± 1 mm in both directions throughout the relevant period. Since an overview of the VENUS detector can be found in our previous report [11], only those features relevant to the present measurement are described in the following.

The central drift chamber (CDC) [14] was the main component for tracking of charged particles. It was a conventional cylindrical multi-wire drift chamber, having a length of about 3 m and a radius of 1.25 m. A total of 29 cylindrical sampling layers, 20 axial layers plus 9 stereo layers, were instrumented. Tracks in a central region, $|\cos\theta| \leq 0.75$, were sampled in all layers, where θ is the polar angle measured from the beam direction. The momentum resolution was $\sigma_p/p = 0.008p_t(\mathrm{GeV}/c)$ for high-momentum ($p_t \gtrsim 5\mathrm{GeV}/c$) particles in the central region, where $p_t = p\sin\theta$. The polar-angle resolution was measured to be $\sigma_{\cot\theta} = 0.008 \pm 0.001$ [11]. The track-extrapolation error at the interaction point was 7 mm along the beam direction and 0.5 mm in the projection onto the transverse plane, for high-momentum particles. The detection efficiency was better than 99.5% per sampling on the average, including the inefficiency due to dead channels.

The flight time of charged particles was measured with time-of-flight (TOF) counters [15]. The TOF system consisted of 96 plastic scintillator rods, arranged in a cylindrical layer at 1.6 m from the beam line. The rods had a cross section of 10.8 cm in width and 4.2 cm in thickness. The gaps between the rods were 3 mm on the average. They had a full length of 4.66 m, covering a polar angle region of $|\cos\theta| \leq 0.81$. The scintillator rods were viewed from both ends by photomultipliers placed outside of the iron yoke, through 1.45 m-long acrylic light guides. Both the timing and the amplitude of the signals were measured. The flight time was reconstructed from the meantime between the two signals from each rod, and corrected for the time walk using the signal amplitude. A time resolution of 200 psec has been achieved for isolated high-momentum particles.

The energy of electrons and photons at large angles, $|\cos\theta| \leq 0.80$, was measured with a cylindrical array of lead-glass (LG) counters [16]. The energy resolution was measured to be 7% for 1.5-GeV electrons from the two-photon process, and 3.8% for 30-GeV electrons from Bhabha scattering.

Eight layers of muon chambers [17] were placed outside of the iron return yoke. In the present measurement, muon-pair events are identified using the event topology, with an energy measurement by the LG counters as a veto. The muon chambers are used for a cross check, because their angular coverage was rather limited.

The data acquisition was triggered by using information on charged-particle tracks in CDC and the TOF counters, together with analog-sum signals from calorimeters. The CDC tracks were reconstructed by a track-finder (TF) circuit [18], and the association of TOF hits was examined by additional trigger-generation circuits. The LG array was subdivided into 58 segments, 8 or 10 segments in the azimuth and 7 segments along the beam direction, providing segment-sum signals as well as a total-sum signal.

Trigger conditions relevant to the detection of muon-pair events were as follows:

(i) A pair of coplanar ($\phi_{\mathrm{acop}} \leq 10°$) CDC tracks were reconstructed by TF, with appropriate association of TOF hits, where ϕ_{acop} is the supplement of the opening angle in the projection onto the plane perpendicular to the beam direction.

(ii) A pair of coplanar ($\phi_{\mathrm{acop}} \leq 30°$) CDC tracks were reconstructed by TF, with an appropriate association of TOF hits.

(iii) Two or more tracks were recognized by TF, and the pulse height of at least one LG segment-sum signal exceeded a threshold, approximately corresponding to 0.7 GeV.

Note that condition (i) was totally contained in condition (ii). Both were retained for a cross check, because the trigger-generation circuits were independent of each other. The main part of muon-pair events was triggered by conditions (i) and (ii). Those events triggered by condition (iii) provided us with information concerning the efficiency of conditions (i) and (ii).

When data acquisition was triggered, digitized data were collected by a FASTBUS processor module, prior to transfer to an online computer. Utilizing the data-collection time, a software selection was applied to those events which were triggered by condition (ii) alone [19]. A tighter association between CDC tracks and TOF hits was required, in order to reduce the events from beam-beam pipe interactions.

B. Luminosity

The integrated luminosity was determined from a measurement of Bhabha scattering at small angles, $14.53° \leq \theta \leq 34.71°$. The experimental procedure is described in detail in our previous report [11], where the experimental precision of 0.7% has been established. The number of events corresponding to the data used for the present measurement is $(1032.6 \pm 7.3) \times 10^3$. Since the luminosity can be given by the ratio of the observed number of events to the cross section of the reaction, what we are left with is to make a reliable theoretical estimation of the cross section. The estimation is described below, emphasizing detailed studies concerning its error.

We used the program ALIBABA [20] for estimating the cross section. This program includes the exact first-order photon-radiation correction and a dominant part (leading-log part) of the second-order corrections, as well as internal electroweak loop corrections. Further higher orders of the photon-radiation correction are partly included by an exponentiation technique.

We defined the signal to be those events in which both e^+ and e^- scattered to a forward region ($14.53° \leq \theta \leq 34.71°$), both had large energies ($E \geq E_{\mathrm{beam}}/3$), and the acollinearity angle between them was smaller than 4° [11]. ALIBABA estimates the cross section for these events to be 3.565 nb, with the input physical parameters, the masses of the Z^0 boson, the top quark and the Higgs boson, chosen to be 91.19, 174 and 300 GeV/c^2, respectively.

The precision of ALIBABA can be evaluated separately for the effective-Born (EB) cross section and the photon-radiation corrections. The technical error in the calculation of the EB cross section, due to possible errors and/or inaccuracy in the program coding, was examined by comparing the result with another calculation independently developed [21]. The difference between them was found to be smaller than 0.1%. The variation due to uncertainties in the input physical parameters, the heavy particle masses, is also negligible.

The largest ambiguity in the EB calculation is in the estimation of the vacuum polarization (self-energy) correction to the photon propagator. While the corrections due to lepton loops are rather trivial, certain ambiguities are present in the hadronic contribution. The hadronic correction is implemented in ALIBABA by using the formula by Burkhardt *et al.*

[22]. The error estimated by Burkhardt *et al.*, about 4% of the correction, leads to an uncertainty in the cross section of 0.15%.

The photon-radiation corrections are dominated by first-order ones. The calculation in ALIBABA can be limited to this order. The exponentiation can also be switched off. The calculation of this setup can be compared with ordinary first-order calculations, providing a good test of the technical precision of the correction. We made a comparison with a program by Tobimatsu and Shimizu (TS program) [23]. The technical precision of the TS program is established to be better than 0.1%, from a comparison with another program, BABAMC [24]. The comparison between ALIBABA and the TS program was made only for the photon-radiation correction by separating it from other corrections, in order to avoid the influence of a difference in internal loop corrections. We found that the difference in the photon-radiation correction is not larger than 0.3% at any scattering angles which we are concerned with.

ALIBABA estimates the first-order photon-radiation correction to be -13.5% for our experimental condition, and the second-order (α^2) leading-log (LL) correction to be $+1.0\%$. The first-order correction can be subdivided into a LL correction of -13.9% and a non-log correction of $+0.4\%$. From these results, assuming a good perturvative behavior in the corrections, we can estimate that the sum of the leading terms among corrections missing in ALIBABA, the α^3-LL correction and the α^2 next-to-leading correction, would be about 0.1% in absolute value. The contribution of further higher orders must be smaller. From these discussions, we assign an error of 0.2% as the uncertainty due to missing higher-order corrections.

The precision of the α^2 correction was examined by comparing the result with that from another program, BHLUM2, in the program package BHLUMI 2.01 [25]. BHLUM2 is a Monte-Carlo event generator including multi-photon radiation effects. The authors of BHLUM2 claim that this program is applicable only to small-angle scattering ($\theta < 10°$). This restriction comes from the absence of corrections to s-channel diagrams and the ignorance of the *up-down* interference. However, with the help of other programs in the BHLUMI package, we confirmed that the inaccuracy due to these approximations is small and can be ignored in the present study.

The comparison was repeated by varying the conditions (the angle cuts, the energy cut as well as the c.m. energy), in order to check the stability of the calculations. Figure 2 shows one of the results, where the difference between the cross-section predictions from the two programs is plotted as a function of the lower angle-cut. We found a systematic difference at the level of 0.2% around the cut for the measurement. The observed difference may be caused by errors in the effective-Born cross section and the first-order corrections that we have already taken into consideration, as well as those in the α^2 correction. It may also be influenced by a difference in the treatment of higher-order corrections. Consequently, we assign an error of 0.3% to the α^2 correction. This must be safe enough because the sum of the errors becomes more than twice the observed systematic difference between ALIBABA and BHLUM2.

It has been pointed out by Caffo *et al.* [26] that the behavior of the α^2-LL correction to the s-t interference part cannot be determined a priori based on the assumptions used for the s-channel and t-channel parts. They concluded that this uncertainty leads to an error of up to 1% at large angles around the Z^0 pole. This estimate is based on the fact that the

interference contribution becomes very large just above the Z^0 peak, nearly -100% at large angles. For our experimental condition, the interference contribution is only -2.5% at the tree level. The uncertainty that Caffo *et al.* pointed out leads to an error of 0.04%. This is negligible in the present study.

The calculation of ALIBABA is performed within the framework of the standard electroweak theory. The estimation may become invalid if there are unexpected interactions. The uncertainty due to such unknown effects is hard to evaluate, and has not been taken into consideration in previous experiments.

In our previous report [11], we examined possible contributions of hypothetical contact interactions [27], using the measured angular distribution of Bhabha-scattering events. The contact interaction can be an effective theory of a wide variety of new interactions, such as compositeness and heavy-particle exchanges. Hence, the obtained limit must be a good estimate for the contribution from unknown phenomena. In Ref. [11] we have established constraints not only for typical combinations of the helicity couplings, which have been assumed by other experiments, but also for arbitrary combinations of them. The result for the latter is suitable for the present study, since new interactions do not necessarily have typical couplings.

The contribution of the contact interaction was examined for 10000 random combinations of the couplings. The coupling strength was set to the maximum value allowed within one standard deviation of the measurement. As a result, we found that the contribution never exceeds 0.25%. We adopt this value for the error due to unknown phenomena. It must be worth mentioning that the allowed contribution is 2.5% at maximum in the large-angle region, $|\cos\theta| \leq 0.743$. This is the reason why we do not use the large-angle measurement for the determination of the luminosity.

Adding all the errors in quadrature, the theoretical error of the calculation by ALIBABA is estimated to be 0.55% for our condition. Together with the experimental error of 0.7%, the total systematic error is evaluated to be 0.9%, yielding the integrated luminosity relevant to the present measurement to be 289.6 ± 2.6 pb^{-1}.

III. EVENT SELECTION

A. Preselection

Muon-pair events were selected from a preselection sample, which mainly consisted of events with low charged-particle multiplicity. The preselection was based on CDC information alone. The applied criteria were as follows:

(P1) The number of tracks reconstructed in CDC was between 2 and 20.

(P2) Among these tracks, at least two tracks satisfied the conditions that $N_{\rm axial} \geq 10$, $N_{\rm stereo} \geq 4$, $|R_{\rm min}| \leq 2.0$ cm, $|Z_{\rm min}| \leq 15.0$ cm and $p_t \geq 0.2$ GeV/c, where $N_{\rm axial}$ and $N_{\rm stereo}$ are the numbers of axial-cell and stereo-cell hits composing the track, respectively. $R_{\rm min}$ is the closest approach to the CDC center axis (z axis), and $Z_{\rm min}$ is the z coordinate there.

(P3) Among the tracks selected in (P2), at least one track satisfied the condition $Q/p \leq 0.5$ (GeV/c)$^{-1}$, where Q is the electric charge of the track ($= \pm 1$).

Condition (P1) sets an upper limit on the multiplicity. Condition (P3) requires the existence of at least one negative-charge or high-momentum ($p_t \geq 2$ GeV/c) track. This requirement efficiently reduced the contamination from beam-beam pipe interactions.

In this preselection we applied a truncated version of the track-reconstruction program in order to save CPU time. The truncation was mainly in the iteration of hit searches, and caused a non-negligible inefficiency in the muon-pair sample, although the selection criteria were looser than the final muon-pair selection. The effect was carefully studied in the estimation of the efficiency.

B. Selection of muon-pair events

After the standard track reconstruction was applied, events in the preselection sample were passed through the final selection to obtain candidates of muon-pair events. The selection criteria were as follows:

(1) The events comprised 2 and only 2 CDC tracks ($N_{\rm track} = 2$). Here, we counted those tracks which satisfied the conditions that $N_{\rm axial} \geq 10$, $N_{\rm stereo} \geq 4$, $|R_{\rm min}| \leq 1.0$ cm, $|Z_{\rm min}| \leq 10$ cm, $p_t \geq 0.2$ GeV/c and $|\cos\theta| \leq 0.8$.

(2) Both tracks were in the central region, $|\cos\theta| \leq 0.75$, and had momenta higher than one half of the beam energy ($p \geq E_{\rm beam}/2$). Furthermore, they had electric charges opposite to each other.

(3) The acollinearity angle between the two tracks, the supplement of the opening angle, was not larger than 10° ($\theta_{\rm acol} \leq 10°$).

(4) The difference in the TOF time between the two tracks was smaller than 5 nsec ($|\Delta t_{\rm TOF}| \leq 5$ nsec).

(5) The total energy in LG was smaller than 5 GeV ($E_{\rm LG} \leq 5$ GeV).

We applied relatively tight requirements on the track information, conditions (1) and (2), while the requirement on the calorimeter energy, condition (5), was rather loose. This choice made the selection insensitive to ambiguous low-energy photon emission. Cosmic-ray events were effectively rejected by condition (4), as shown in Fig. 3. Condition (5) rejected Bhabha-scattering events. It should be noted that no constraint was set on charged-particle tracks and calorimeter energies at small angles, $|\cos\theta| > 0.8$.

A total of 4484 events were selected under these criteria. The obtained sample was subdivided into six bins, according to the cosine of the production angle (θ) defined by the angle between the negative-charge track (μ^-) and the incoming electron (e^-) beam. The contents in the bins are listed in Table I.

IV. CORRECTIONS

A. Definition of the signal

We have to give an explicit definition of the signal events, in order to make the experimental result comparable with theoretical predictions. In the present measurement, we define the signal to be those events from reaction (2), in which both muons are produced at large angles ($|\cos\theta| \leq 0.75$) with high momenta ($p \geq E_{\rm beam}/2$), and satisfy the collinearity

condition, $\theta_{\rm acol} \leq 10°$. The constraints are defined only for the muon pair, while no explicit requirement is imposed to the photon radiation.

The background contamination and the detection efficiency were estimated according to this definition. These corrections were estimated independently in the angular bins as far as possible. Independent estimations were, however, impossible in some cases. In such cases, estimated errors have certain correlations between the bins. These correlations were treated in the form of an error (covariance) matrix [11].

B. Background contamination

The background is expected to be dominated by the contamination of tau-pair events from the $e^+e^- \to \tau^+\tau^-$ reaction, and muon-pair events from the $e^+e^- \to e^+e^-\mu^+\mu^-$ reaction. The contributions of these reactions were estimated by means of Monte-Carlo simulations.

The tau-pair events were generated using a program including the first-order radiative correction [28]. The generated events were passed through a full detector simulator, after the tau leptons were forced to decay through JETSET 7.3 [29]. Applying the event selection to these events, we found the contamination to be 29.5 ± 2.5 events, corresponding to (0.66 ± 0.06)% of the muon-pair candidates. The error originates from the statistics of the simulation. We assigned an additional overall error, 10% of the estimated contamination, in order to take account of the uncertainties in the decay branching ratios and the detector simulation. The effect of the tau polarization was evaluated by using another event generator [30]. We found that the effect is smaller than 1% of the estimated contamination, even if the polarization allowed by our measurement [31] is taken into consideration.

The contamination from the $e^+e^-\mu^+\mu^-$ events was estimated by using an event generator based on the lowest-order QED calculation [32], to be 14.1 ± 1.3 events. The simulation shows that the contribution of the *conversion* diagrams is dominant, where the initial-state e^+e^- pair annihilates to two virtual photons, and they *convert* to an e^+e^- pair and a $\mu^+\mu^-$ pair. Since a large invariant mass is required for the muon pair in the event selection effectively, the electroweak (Z^0 exchange) effect ignored in the simulation may be appreciable. The effect would show up as a forward-backward (FB) asymmetry of the contamination. The angular distribution of the contamination was estimated by taking this into consideration.

We took the average between the simulation result, which is FB symmetric by definition, and a distribution rearranged to give the same FB asymmetry as the muon-pair candidates. The difference between the average and the simulation was taken to be an error. This error is fully correlated between the angular bins, and contributes to the error in the angular distribution only. In addition, an overall error, 10% of the estimated contamination, was assigned in order to take account of the effect of radiative corrections ignored in the simulation.

The contamination of cosmic-ray events was estimated from the distribution of the event vertex along the beam direction ($z_{\rm evt}$). The event vertex was determined from the average of the z intercepts ($Z_{\rm min}$) of the two muon tracks. The distribution for the muon-pair candidates is plotted in Fig. 4, and compared with that for cosmic-ray events identified from the TOF difference. The candidates are concentrated in a narrow region, while the cosmic-ray events show a flat distribution.

The contamination was estimated from the events (6 events) outside of the region, $-4 \leq$

$z_{\rm evt} \leq 5$ cm. These events, except for one event, were confirmed to be cosmic-ray events; the event vertices in the x-y projection are simultaneously distant from the average interaction point. They would have been selected due to accidental coincidences with X-ray or other cosmic-ray hits in the TOF counters. One event was likely to be a muon-pair event, with one track having bad quality in the z reconstruction. By extrapolating the five identified events, the total contamination of cosmic-ray events was estimated to be 10.2 ± 2.3 events.

Bhabha scattering events can contaminate the muon-pair sample only if both electrons hit dead LG counters, because there was no gap in the LG array. This contamination was very small because dead counters distributed sparsely and any pair of them was not in back-to-back positions. The contamination was numerically estimated by counting the LG-counter hits. The number of counters, having energies more than 50 MeV, was counted in a 3×3 array around the extrapolation of CDC tracks. Among the two numbers corresponding to the two tracks in each event, the smaller one ($N_{\rm LG}^{\rm smaller}$) was a good measure for this study.

For Bhabha scattering events, $N_{\rm LG}^{\rm smaller}$ was large because of the presence of a lateral spread of the electromagnetic shower. We found that $N_{\rm LG}^{\rm smaller} \geq 5$ for 83% of those events which satisfy the criteria for the muon-pair selection, if the highest-energy counters in both 3×3 arrays are discarded. Thus, we can expect that 83% of the contaminating events are in the region $N_{\rm LG}^{\rm smaller} \geq 4$. On the other hand, $N_{\rm LG}^{\rm smaller}$ was very small for the muon-pair candidates. It was equal to 1 for about 90% of the events, 2 for most of the others, and 3 for only three events. There was no event in the region $N_{\rm LG}^{\rm smaller} \geq 4$. From these results, we can estimate that the contamination in the region $N_{\rm LG}^{\rm smaller} \leq 3$, where the muon-pair candidates distribute, is less than 0.6 event at the 95% confidence level. Such a small contamination can be ignored.

C. Detection efficiency

1. Track reconstruction

The track-reconstruction capability was examined by using a sample of muon-pair events, selected without depending on detailed performance of CDC and the reconstruction program. In this study, CDC tracks were reconstructed by looking for rows of hit drift-cells corresponding to high-momentum tracks, without using drift-time information. The track parameters were determined from the positions of the sense wires. The small cell arrangement of CDC and the low track-multiplicity of the events of interest allowed us to carry out this analysis with sufficient performance. The event inefficiency for two-track events was found to be smaller than 0.1%, by applying the analysis to simulation events and Bhabha-scattering events. The track extrapolation error was about 1 cm at the TOF counters in the x-y projection. The reconstruction was performed in three dimensions.

The analysis was applied to about one third of all data before the preselection. We selected those events in which two and only two tracks were reconstructed. The average curvature of the two tracks was required to be smaller than 0.02 $\rm m^{-1}$ in the x-y projection. This cut corresponds to a p_t cut of about 10 GeV/c. The other requirements concerning the acollinearity, the TOF difference and the LG energy were the same as in the standard selection. About 1700 events remained after the selection. The momentum spectrum of the

tracks indicates that the contamination from other processes, including cosmic rays, was less than 10%.

We applied the standard track reconstruction to the selected events, and found that the event inefficiency due to the tracking failure was (0.17 ± 0.10)%. We found that one of the tracks was successfully reconstructed, and that there was a clear row of CDC hits in the direction opposite to the reconstructed track, even in the inefficient events (3 events). These indicate that they are not contamination, but muon-pair events. Therefore, the contribution of the contamination in the event sample can be ignored in this estimate. We could not find any apparent reason for this failure.

It should be noted that the above estimate on the tracking failure is substantially smaller than that for Bhabha-scattering events, (0.4 ± 0.1)% [11]. The tracking capability for electrons must have been affected by their interactions in the detector materials.

As has been mentioned, we adopted a truncated version of the track reconstruction in the preselection. The inefficiency due to the truncation was estimated using the above event sample. By applying the standard muon-pair selection to these events, we were left with about 1600 muon-pair events. The truncated reconstruction and the preselection were then applied to them. As a result, we found that the inefficiency due to the preselection was (1.73 ± 0.33)%. Adding the two estimates, the total inefficiency relevant to the track reconstruction is estimated to be (1.90 ± 0.34)%. The estimated inefficiency does not show any significant angular dependence.

2. Charge misidentification

In the event selection, 25 events were rejected because the reconstructed two tracks had the same sign of the electric charge; *i.e.*, the charge was misidentified for one of the tracks. The inefficiency due to this selection is 0.55% for the total yield without any ambiguity, since we know the exact number. However, there is an ambiguity in the angular dependence.

Since the two tracks are nearly back-to-back, we can determine the absolute value of $\cos\theta$ even for the same-charge events. The inefficiency can therefore be determined as a function of $|\cos\theta|$. The estimated inefficiency shows a significant $|\cos\theta|$ dependence; it is 1.05% for $|\cos\theta| < 0.25$, 0.42% for $0.25 < |\cos\theta| < 0.50$, and 0.29% for $0.50 < |\cos\theta| < 0.75$. This is reasonable since the misidentification probability should increase as p_t becomes larger.

The inefficiency for the correction was determined by assuming a forward-backward symmetry. Since the events consist of nearly back-to-back two tracks, the asymmetry in the inefficiency can emerge only if the misidentification probability has a certain charge asymmetry and, in addition, this charge asymmetry has an appreciable forward-backward asymmetry. It is hard to believe that such an effect was significant, since we did not observe any significant charge dependence in track qualities.

The error of this inefficiency was determined conservatively, since we do not have any direct evidence supporting the assumption. We assigned the error so that it should amount to 100% of the estimated inefficiency in the forward ($\cos\theta > 0$) bins. This error has a full negative correlation between the corresponding forward and backward bins, since it should never contribute to the error in the total yield or the total cross section.

3. Track resolution

The inefficiency due to finite resolutions in the track measurement was evaluated by using Monte-Carlo event simulations. A program including the full electroweak order-α correction, coded by Fujimoto and Shimizu (FS program) [28], was mainly used for event generation. The generated events were passed through a simple detector simulation, where the polar angle ($\cot\theta$) and $1/p_t$ of the muons were smeared according to the known resolutions, assuming Gaussian distributions. The acollinearity angle distribution after the smearing is compared with that of the candidate events in Fig. 5. The simulation well reproduces the data at large angles relevant to the selection.

As a result of the smearing, some signal events go out of the selection criteria, and some non-signal events come into the criteria. In order to simplify the discussion, we define the efficiency to be the ratio of the number of candidate events after smearing to the number of signal events.

From this study, we found that the inefficiency due to the $\cot\theta$ resolution is very small, $(0.13 \pm 0.03)\%$. The effects of possible shifts in the angle measurement, $|\Delta\cot\theta/\cot\theta| < 1.3\times10^{-3}$ or $|\Delta\cot\theta| < 10^{-3}$ [11], were found to be even smaller, less than 0.1%, and able to be ignored in all bins.

This simulation was found to be insufficient for studying the momentum resolution effects. We observed a substantial deficit of the simulation in the momentum spectrum at low momenta near to the threshold. The improvement was not significant even if we used another event generator, KORALZ [30], including multi-photon emission. The discrepancy is, therefore, considered to have been caused by a non-Gaussian response of the momentum measurement.

Figure 6 shows the momentum spectrum for the lower-momentum tracks ($p_{\rm lower}$) relevant to the momentum cut. In this plot, the momentum cut was lowered to $E_{\rm beam}/4$, in order to look at the behavior around and below the threshold. The simulation spectrum was obtained by using KORALZ, together with a full detector simulator in which the track-distance dependence of the CDC resolution is simulated. Although this simulation reasonably reproduces a non-Gaussian behavior around the peak, it is not enough to explain the tail extending below the threshold. Any effect missing in the simulation, such as X-ray background from the beams, would have affected the measurement. By the way, the excess of data is small below the threshold, and the spectrum at very low momenta, $p_{\rm lower}/E_{\rm beam} \lesssim 1/3$, is in good agreement with the expected background contribution.

We estimated the inefficiency due to this tail from the difference between the data and the simulation (including the background) below the threshold, $0.25 \le p_{\rm lower}/E_{\rm beam} < 0.5$. Adding the inefficiency from the KORALZ simulation (0.12%), we estimated the inefficiency due to the momentum cut to be $(0.64\pm0.33)\%$. We assigned an additional overall systematic error of 0.26% to this estimate. This error, which corresponds to one half of the observed difference at low momenta, was added because some part of the difference may be due to higher-order effects still missing in KORALZ.

It should be noted that in Fig. 6 we have chosen a distribution which enhances the difference between the data and the simulation, in order to make the small difference visible. We can realize that the difference is very small if we chose another distribution, the $1/p$ spectrum, shown in Fig. 7. The excess of data near to the threshold in Fig. 6 corresponds

to a shallow tail at around $E_{\rm beam}/p = 2$. The selection of the lower-momentum tracks is an additional bias leading to the enhancement. Together with a slight difference in the non-Gaussian behavior around the peak, this selection generates a shift of the peak position, which we can see in Fig. 6. We cannot find such a shift in the unbiased $1/p$ spectrum in Fig. 7.

It should also be worth noticing that we can also see a tail in the small $1/p$ side in Fig. 7. This tail should extend below $1/p = 0$ and cause charge misidentification. Since, ignoring the photon-radiation effect, the $1/p$ spectrum should be symmetric with respect to the peak, the number of the signal events in the region $1/p > 2$ should be approximately the same as that in $1/p < 0$. Therefore, the fact that the inefficiency estimated here is nearly the same as the inefficiency due to charge misidentification is evidence for the reliability of the above estimation.

4. Multi-track events

The signal events may have been discarded if additional tracks were produced from the conversion of photons emitted in association with muon-pair production. The corresponding inefficiency was studied by using a muon-pair sample collected with a looser requirement on the number of tracks. We required that the events should include two or more tracks, and at least one of the pairs of these tracks should satisfy the requirements in the standard selection. The selected sample contained 56 multi-track ($N_{\rm track} \ge 3$) events, in addition to the 4484 events in the standard sample. There was no event that contained more than two high-momentum tracks.

We visually inspected these multi-track events, and found that 39 events among them were obviously muon-pair events associated with converted photons. In these events, clear muon-chamber hits were observed around the extrapolation of high-momentum tracks, and additional low-momentum tracks seemed to be electrons from the LG response. The identification was ambiguous for the rest of the events (17 events), though some of them looked like contamination from other processes, such as tau-pairs and $\mu^+\mu^-$+hadrons events. From these observations, we conservatively estimated that the loss due to the tight requirement on the number of tracks was 47.5 ± 8.5 events. This corresponds to a signal inefficiency of $(1.1 \pm 0.2)\%$.

5. TOF efficiency

The main reason for the TOF inefficiency was the gaps between the counters. Since the fraction of gaps was about 3% of the whole coverage, the event inefficiency due to them is estimated to be about 6%, naively. It is one of the dominant corrections in the present measurement. The inefficiency was carefully studied by using real data, because the response to those muons passing near to the edges of the counters is ambiguous.

Bhabha-scattering events have been used by many experiments to study the TOF-counter efficiency. However, for the same reason as in the study of the tracking efficiency, estimates based on them may not be appropriate for muon-pair events. Actually, we obtained an event inefficiency of 2% from Bhabha-scattering events. This is obviously smaller than the naive

estimate. The interactions of the electrons in the detector materials would have increased the efficiency.

As has been described, trigger-condition (iii) did not require any TOF hits, and about 65% of the muon-pair candidates were triggered by this mode as well as conditions (i) and (ii). Those events triggered by this mode are, therefore, suitable for studying the TOF efficiency. The sample events were selected from the preselection sample. The standard muon-pair selection, except for the requirement on the TOF information, was then applied to them.

Since TOF matching was not required, the sample had a large contamination from cosmic rays. In order to reduce them, we required that both tracks were reconstructed with good quality; $N_{\rm axial} \geq 16$, $N_{\rm stereo} \geq 7$, $|R_{\rm min}| \leq 0.2$ cm and the reduced χ^2 be smaller than 4.0 in both x-y and z reconstructions. Finally, the z vertex of the event ($z_{\rm evt}$) was required to be in the range $-4.0 \leq z_{\rm evt} \leq 5.0$ cm. Although these requirements are tighter than those in the standard selection, they are loose enough to accept muon-pair events.

A total of 2531 events were selected from the whole preselection sample. The contamination of cosmic-ray events was estimated to be 47 ± 7 events, from the number of events rejected by the $z_{\rm evt}$ cut. The TOF-hit association was examined for the selected events. We found that one of the tracks was not connected to any TOF hit in 125 events. There was no event in which both tracks missed the hits. From this result, we estimate the event inefficiency due to the lack of the TOF-hit connection to be $(4.94 \pm 0.43)\%$. The contamination of cosmic rays can be ignored, because there was no enhancement of them in the inefficient events.

This result is consistent with the naive estimate. Small tilts of the tracks due to the bend by the magnetic field would have slightly reduced the gap effect. For a confirmation, we investigated the expected injection points to the TOF counters for the tracks that were not connected to TOF hits. We found that the injection points were all concentrated around the counter boundaries.

Even if the tracks were connected to TOF hits, events were rejected if the TOF difference exceeded the selection criterion, $|\Delta t_{\rm TOF}| \leq 5$ nsec. This may happen if either hit was affected by accidental hits of X rays or cosmic rays preceding the muon hits. This effect was investigated by using those events in which both tracks were connected to TOF hits in the above sample. The cosmic-ray contamination was further reduced by requiring that at least one of the tracks was connected to a TOF hit with a good timing quantity; the measured time was required to be within 1.0 nsec from that expected from the track path length.

Among 2369 events which remained after the selection, eight events did not satisfy the $|\Delta t_{\rm TOF}|$ requirement. From the $z_{\rm evt}$ distribution, the remaining cosmic-ray contamination was estimated to be 6.2 ± 2.5 events. The number of large $|\Delta t_{\rm TOF}|$ events is consistent with this value. The inefficiency for the muon-pair events was estimated from the difference between these results to be $(0.08 \pm 0.16)\%$.

If the large $|\Delta t_{\rm TOF}|$ is caused by any accidental coincidence, similar effects must also be seen in Bhabha-scattering events. The $|\Delta t_{\rm TOF}|$ distribution for a sample of Bhabha-scattering events is overwritten in Fig. 3. We can see a good agreement with the distribution for the muon-pair events. The inefficiency estimated from the Bhabha-event spectrum (0.12%) is in good agreement with the above estimate.

The total inefficiency due to the TOF requirements is then estimated to be $(5.02 \pm 0.46)\%$.

We did not observe any significant $\cos\theta$-dependence in this inefficiency.

6. LG-energy cut

In the definition of the signal events, we did not impose any explicit constraint on the photon radiation, in order to avoid theoretical ambiguities associated with it. As a drawback, we have to account for the rejection of the signal events by the condition $E_{\rm LG} \leq 5$ GeV to be a source of inefficiency.

This inefficiency was studied by using a sample of muon-pair events, identified from the muon-chamber information instead of the LG energy. We required that both tracks were identified as muons, with the association of at least three muon-chamber hits around the extrapolation of each track. The other criteria for the selection were the same as those in the standard selection. We examined the LG energy in the selected events, and found that $(4.80 \pm 0.35)\%$ of the events were to be rejected by the LG-energy cut. This estimate cannot be adopted for the correction directly, since the production angle of the used events was limited to $|\cos\theta| \lesssim 0.6$, because of the limited coverage of the muon chambers.

Along with the above study, we carried out a simulation study using the FS program. The energy of photons within the acceptance of LG was smeared according to the measurement resolution. The LG response to muons was simulated so that the single-muon response should be reasonably reproduced. An exponential tail extending to higher energies from the muon peak, possibly due to the delta-ray emission by muons, was also simulated. The inefficiency due to the LG-energy cut was estimated to be 4.56% from this simulation. This is in good agreement with the estimate based on data.

The simulated LG-energy spectrum is compared with that for the candidate events in Fig. 8. We can see that the muon contribution, including the tail, is overwhelmed by hard-photon radiations at high energies around the cut. The simulation is in excellent agreement with the data there. From this simulation, we found that the dependence of the inefficiency on the muon-pair production angle is not significant, less than $\pm 0.2\%$ over the acceptance.

For the correction of the data, we adopt the estimate from data, $(4.80 \pm 0.35)\%$, to all angular bins. The error is considered to be an overall ambiguity. We assign an additional bin-by-bin error of 0.2%, in order to take into account possible angular dependence allowed by the simulation result. The effect of the photon radiation should be forward-backward symmetric, since the radiation does not depend on the sign of the charges of the particles. The bin-by-bin error is therefore assumed to have a full positive correlation between the bins having the same $|\cos\theta|$.

7. Event trigger

All of the selected muon-pair candidates were found to be triggered by trigger-condition (i). This trigger was generated from the CDC track information provided by the track finder (TF) and the hit pattern of the TOF counters. The efficiency relevant to the TOF hits has already been evaluated. The subject in this subsection is to evaluate the efficiency of the other parts, TF and additional circuits for trigger generation.

The efficiency concerning the trigger-generation circuit was investigated by using the event sample that had been used to study the TOF efficiency, for which trigger (iii) was issued and both tracks were associated with TOF hits. We found that trigger (i) was issued in all 2531 events. Since the trigger-generation circuits were independent of each other for these triggers, we can estimate the inefficiency to be smaller than 0.1%. This is small and can be ignored, compared to other inefficiencies.

The efficiency of TF was estimated by using a sample of clean Bhabha events. Since only the behavior of particles in the tracking volume of CDC is relevant to the TF performance, the difference between the muons and the electrons is expected to be insignificant if appropriately clean events are selected. We required the same criteria that had been applied to the sample events for studying the $|\Delta t_{\rm TOF}|$ efficiency, except for the requirements on the event trigger and the LG energy. Instead of the excluded criteria, we required that the events were triggered by the LG total-energy trigger and had large energy deposits in LG, $E_{\rm LG} \geq 0.8\sqrt{s}$.

Since at least two LG segment-sum signals exceed the threshold in these events, the fraction of those events in which trigger (iii) was simultaneously issued gives an estimate of the TF efficiency. From this study, the inefficiency was found to be $(0.19 \pm 0.02)\%$. The main reason for the inefficiency was found to be the existence of a dead CDC channel in a relatively less redundant part in the preloaded trigger pattern of TF. Some part of the inefficiency was due to an instability of one of the TF channels which had not been recognized during the experiment. In any case, the observed inefficiency is very small. We assign a common inefficiency of 0.19% to all $\cos\theta$ bins and ignore the error.

D. Consistency between the data samples

The consistency between data samples, from which the muon-pair events and the small-angle Bhabha scattering events used for the luminosity measurement were selected, is not trivial. The muon-pair preselection sample was obtained after several steps of the selection procedure. On the other hand, the Bhabha-scattering events were selected in a semi-online analysis, carried out in parallel to the data acquisition. We need to apply additional corrections, if any serious mistakes were made in these processes.

The consistency was examined by comparing large-angle Bhabha scattering events. These events were simultaneously selected in the semi-online analysis, and remained in the muon-pair preselection. However, the comparison could not be done directly because of the existence of a slight incompatibility in the event analysis, mainly due to options in the CDC track reconstruction.

The comparison was mediated by another preselection sample from which the final sample of large-angle Bhabha scattering events was selected, because full event data were not available as the result of the semi-online analysis. The consistency between the two preselection samples was tested by applying additional selections to both of them, so that the selection conditions, including the track-reconstruction options, should become exactly identical. The comparison between the Bhabha preselection sample and the data passed through the semi-online analysis was straightforward, because the selection conditions for large-angle Bhabha events were identical in these two procedures.

The studies were carried out by checking the event-by-event matching. As a result, we found a certain inconsistency between the samples. The inconsistency was apparently due to mistakes in the selection processes; some runs have been dropped from one of the samples, and some from another. However, the inconsistency was found to be very small, less than 0.05% of the whole data. Thus, we do not apply any correction for it.

E. Result

The individual estimates of the background contamination were summed to obtain the total bin-by-bin contamination ($N_i^{\rm bkg}$). The estimates of the inefficiency were first converted to their supplements, partial efficiencies; then, their product was calculated to obtain the bin-by-bin efficiency (ε_i). These results are listed in Table I, where the obtained bin-by-bin efficiency is shown in terms of the inefficiency $(1-\varepsilon_i)$.

The number of candidates (N_i) was converted to the binned signal cross section ($\sigma_i^{\rm signal}$) according to the formula,

$$\sigma_i^{\rm signal} = \frac{N_i - N_i^{\rm bkg}}{\varepsilon_i L}, \tag{3}$$

where L is the integrated luminosity. The result is shown in Table I. The quoted error includes the error of the luminosity, as well as those from the data statistics and the corrections. The correlation matrix for the error, the non-dimensional element of the error matrix, is given in Table II.

From a sum of the binned cross section, the backward ($\cos\theta < 0$) and forward ($\cos\theta > 0$) cross sections for the signal events are obtained as:

$$\begin{aligned} \sigma_{\rm B}^{\rm signal} &= 11.09 \pm 0.26 \text{ pb}, \\ \sigma_{\rm F}^{\rm signal} &= 6.59 \pm 0.20 \text{ pb}, \end{aligned} \tag{4}$$

with the error correlation of 0.113. This result can be converted to the total cross section and the forward-backward (FB) asymmetry, according to the following definition:

$$\sigma = \sigma_{\rm F} + \sigma_{\rm B}, \quad A_{\rm FB} = \frac{\sigma_{\rm F} - \sigma_{\rm B}}{\sigma_{\rm F} + \sigma_{\rm B}}. \tag{5}$$

The result is:

$$\begin{aligned} \sigma^{\rm signal} &= 17.69 \pm 0.35 \text{ pb}, \\ A_{\rm FB}^{\rm signal} &= -0.254 \pm 0.017. \end{aligned} \tag{6}$$

The error correlation is small, -0.011, in this result.

In Eq. (6), the total cross section has been measured with a precision of 2.0%. Among various sources of the error, dominating is the data statistics (1.5%). Others are 0.9% from the uncertainty in the efficiency and another 0.9% from the luminosity measurement. The contribution of the uncertainty in the background contamination is very small (0.12%). The error of the FB asymmetry is also dominated by the data statistics, 0.014 out of 0.017.

Another 0.01 mainly originates from the uncertainty in the angular dependence of the efficiency.

It should be noted that the measurement results obtained in this section are independent of any models or theories describing the reaction. Some of the corrections have been estimated using simulations based on the standard theory. However, the dependence on the theory can be ignored, since these corrections are very small. The dominant corrections were determined based on analyses of real events.

V. DISCUSSIONS

A. Comparison with the standard electroweak theory

The prediction of the standard electroweak theory was calculated using the computer program ALIBABA [20]. This program is a semi-analytical calculation, including photon-radiation corrections up to α^2 leading-log terms, as well as internal electroweak corrections. This is the same program that has been used for determining the luminosity. Although the main purpose of ALIBABA is to calculate the Bhabha scattering cross section, it can reliably evaluate other fermion-pair productions by switching off the t-channel contributions. The precision of the calculation is expected to be better than 1% for the muon-pair production at our energy. An additional advantage of this program is that it can calculate the prediction under the same condition that we have adopted for the definition of signal events.

ALIBABA gives the total cross section and the forward-backward (FB) asymmetry for the signal events, defined by Eq. (5), as:

$$\sigma^{\rm signal} = 18.07 \text{ pb}, \quad A_{\rm FB}^{\rm signal} = -0.258, \tag{7}$$

for the input Z^0, top-quark, and Higgs-boson masses of 91.19, 174, and 300 GeV/c^2, respectively. This is to be compared with the experimental result of Eq. (6). We can see that the result of the present measurement has the same trend that has been observed in measurements at lower energies; that is, the total cross section tends to be smaller than the prediction, while the FB asymmetry is in good agreement [9,10]. However, the difference in the total cross section is only 1.1-times the estimated error in the present result. As for the FB asymmetry, the agreement is very good. The difference is only 0.2-times the error.

The binned cross section given by ALIBABA is listed in the last column of Table I, and compared with the experimental result in Fig. 9. We cannot find any apparent difference. The χ^2 is evaluated to be 5.15 for 6 degrees of freedom, from the error in Table I together with the correlation matrix in Table II. Namely, the experimental result and the prediction are in good agreement.

Comparisons were also made with other programs based on the standard electroweak theory, ZFITTER [33] and KORALZ [30]. They are expected to have a precision comparable to ALIBABA. The results are summarized in Table III. In the calculation with ZFITTER, the explicit angular-acceptance cut can be applied to either μ^- or μ^+, while the other constraints in our signal definition can be directly imposed. The correction corresponding to this difference was estimated using ALIBABA and applied to the experimental result. The corrected results are denoted by the superscript ZF in Table III.

On the other hand, we can impose any constraints to KORALZ, since it is an event generator. The calculation was done for both our signal definition and the ZF definition. However, the comparison is done only for the total cross section, because KORALZ does not include the interference between the photon radiations from the initial state and the final state. The interference results in a shift of about 0.02 in the FB asymmetry in the order-α correction for our condition.

The theoretical predictions are in very good agreement with each other, except for a small, but appreciable, difference between ZFITTER and the others in the total cross section. The discrepancy between ALIBABA and ZFITTER has been known for long time [33]. Because the agreement between ALIBABA and KORALZ is quite good, this difference is likely to be due to a certain inaccuracy in ZFITTER. An over-simplification of the radiator function might be the reason. By the way, the difference (0.8%) is smaller than the experimental error and the theoretical predictions are all consistent with the experimental result.

B. Effective-Born cross section

The cross sections of reactions in e^+e^- collisions can be described with effective-Born (EB) cross sections representing short-range hard interactions, and photon-radiation corrections applied to them by convolution [20,33]. In the present measurement, the contribution of the radiation of highly energetic photons is effectively suppressed by the constraints on the produced muons. Furthermore, the EB cross section is not expected to have any apparent structure near to the c.m. energy. In such a case, the convolution can be approximated by a factorized correction as

$$\sigma = (1 + \delta^{\rm rad})\sigma^{\rm EB}, \tag{8}$$

where $\sigma^{\rm EB}$ denotes the effective-Born cross section and σ is the cross section to be measured.

The measured signal cross section ($\sigma_i^{\rm signal}$) was converted to the binned EB cross section ($\sigma_i^{\rm EB}$) using this approximation. The correction factor $\delta^{\rm rad}$ was estimated by using ALIBABA, as shown in Table IV. From a sum of the obtained EB cross section, we can evaluate the total cross section and the FB asymmetry for our angular coverage, $|\cos\theta| \leq 0.75$, as:

$$\begin{aligned} \sigma^{\rm EB}(0.75) &= 20.11 \pm 0.39 \text{ pb}, \\ A_{\rm FB}^{\rm EB}(0.75) &= -0.280 \pm 0.017, \end{aligned} \tag{9}$$

with the error correlation of -0.011. The predictions from the theoretical calculations are summarized in Table III. They are in very good agreement with each other and consistent with the experimental result.

The binned EB cross section was further converted to the differential cross section at the center of the $\cos\theta$ bins ($\cos\theta_i$), according to the formula

$$\frac{d\sigma_i^{\rm EB}}{d\Omega} = \frac{\sigma_i^{\rm EB}}{2\pi\Delta\cos\theta(1+\delta_i^{\rm bin})}, \tag{10}$$

where $\Delta\cos\theta$ is the bin width ($= 0.25$) and $\delta_i^{\rm bin}$ is the correction for the binning effect, the difference between the average and the center value. This correction was estimated from the EB cross section given by ALIBABA, and found to be very small as shown in Table IV.

The obtained differential cross section is presented in Table IV and plotted in Fig. 10. Since the EB cross section is relevant to the non-radiative reaction, reaction (1), the differential cross section should be described as

$$\frac{d\sigma^{\rm EB}}{d\Omega} = \frac{\sigma^{\rm EB}_{\rm TOT}}{2\pi}\left\{\frac{3}{8}\left(1+\cos^2\theta\right) + A^{\rm EB}_{\rm FB}\cos\theta\right\}, \tag{11}$$

if the reaction originates from helicity-conserving interactions only. The parameters $\sigma^{\rm EB}_{\rm TOT}$ and $A^{\rm EB}_{\rm FB}$ correspond to the cross section and the FB asymmetry for the full solid angle, respectively.

Fitting Eq. (11) to the measured differential cross section, we obtain the parameters as:

$$\begin{aligned}\sigma^{\rm EB}_{\rm TOT} &= 30.05 \pm 0.59 \text{ pb},\\ A^{\rm EB}_{\rm FB} &= -0.350 \pm 0.017\ .\end{aligned} \tag{12}$$

The error correlation is -0.034. This result is consistent with the prediction from ALIBABA, $\sigma^{\rm EB}_{\rm TOT} = 30.74$ pb and $A^{\rm EB}_{\rm FB} = -0.338$, obtained by extrapolating the prediction in Table III to the full solid angle according to Eq. (11). The result in Eq. (12) corresponds to the quantities within the acceptance ($|\cos\theta| \le 0.75$) as $\sigma^{\rm EB}(0.75) = 20.07 \pm 0.39$ pb and $A^{\rm EB}_{\rm FB}(0.75) = -0.295 \pm 0.014$. This is in good agreement with the result from the sum of the binned cross sections, Eq. (9). This agreement indicates the validity of the assumption of Eq. (11).

Up to here, we have compared the result from the present measurement with the prediction of the standard electroweak theory from various aspects, and found reasonable agreement between them. The agreement has been confirmed not only in the global behavior, the total cross section and the FB asymmetry, but also in the more-detailed production-angle distribution. In the following subsections we examine the sensitivity of the measurement to the underlying physics by introducing some extensions from the standard theory. The sensitivity is evaluated in terms of the constraints to the extensions.

C. S-matrix method

The S-matrix method [34] has been proposed as one of the most general ways in model-independent approaches to evaluate the validity of the standard theory. The measurable quantities are described with phenomenological parameters, independent of the constraints from the standard theory. In the simplest parametrization of the S-matrix method, the total cross section and the FB asymmetry are described as:

$$\begin{aligned}\sigma^{\rm EB}_{\rm TOT} &= \frac{4}{3}\pi\alpha^2\left\{\frac{r^\gamma_{\rm tot}}{s} + \frac{s r_{\rm tot} + (s-\overline{m}_Z^2)j_{\rm tot}}{(s-\overline{m}_Z^2)^2 + \overline{m}_Z^2\overline{\Gamma}_Z^2}\right\},\\ \sigma^{\rm EB}_{\rm FB} &= \pi\alpha^2\left\{\frac{r^\gamma_{\rm fb}}{s} + \frac{s r_{\rm fb} + (s-\overline{m}_Z^2)j_{\rm fb}}{(s-\overline{m}_Z^2)^2 + \overline{m}_Z^2\overline{\Gamma}_Z^2}\right\},\end{aligned} \tag{13}$$

and $A^{\rm EB}_{\rm FB} = \sigma^{\rm EB}_{\rm FB}/\sigma^{\rm EB}_{\rm TOT}$. The resonance parameters are given by the Z^0 mass and width in the standard definition as $\overline{m}_Z = m_Z - 34$ MeV and $\overline{\Gamma}_Z = \Gamma_Z - 1$ MeV. The r^γ and r parameters represent the direct contribution of the photon and Z^0 exchanges, respectively, and the interference between them is described by the j parameters.

If the standard theory is valid, the parameters for the muon-pair production can be described as:

$$\begin{aligned} r^\gamma_{\rm tot} &= \left(\frac{\alpha(s)}{\alpha}\right)^2, \quad r^\gamma_{\rm fb} = 0,\\ r_{\rm tot} &= \left(\frac{\alpha_Z}{\alpha}\right)^2 (a_\ell^2+v_\ell^2)^2, \quad r_{\rm fb} = 4\left(\frac{\alpha_Z}{\alpha}\right)^2 a_\ell^2 v_\ell^2,\\ j_{\rm tot} &= 2\frac{\alpha(s)}{\alpha}\frac{\alpha_Z}{\alpha}v_\ell^2, \quad j_{\rm fb} = 2\frac{\alpha(s)}{\alpha}\frac{\alpha_Z}{\alpha}a_\ell^2,\end{aligned} \tag{14}$$

based on the improved-Born approximation [35]. The parameter $\alpha(s)$ is the so-called running QED coupling, and $\alpha(s)/\alpha = 1.059$ at $\sqrt{s} = 57.77$ GeV. The parameter α_Z is given as

$$\frac{\alpha_Z}{\alpha} = \frac{m_Z^2}{4A_0}\rho \tag{15}$$

with $A_0 = (37.28\ \text{GeV})^2$. The ρ parameter is 1.010 if the correction due to the large top-quark mass (174 GeV/c^2) is taken into account. The effective axial-vector and vector coupling parameters for charged leptons are given as:

$$a_\ell = -\frac{1}{2}, \quad v_\ell = a_\ell + 2\sin^2\theta^{\rm eff}_W. \tag{16}$$

Using these relations, Eq. (13) gives the total cross section and the FB asymmetry as $\sigma^{\rm EB}_{\rm TOT} = 30.77$ pb and $A^{\rm EB}_{\rm FB} = -0.339$, for $m_Z = 91.19$ GeV/c^2, $\Gamma_Z = 2.50$ GeV and $\sin^2\theta^{\rm eff}_W = 0.232$. They are in good agreement with the prediction of ALIBABA.

Among many parameters in the S-matrix method, those for the photon exchange (r^γ) are well known from low-energy experiments and phenomenological calculations. The Z^0-exchange interactions have been precisely measured by experiments in the resonance region, and good agreement with the standard theory has been established. Measurements at TRISTAN energies are expected to be sensitive to the interference between them. Therefore, it must be reasonable to assume the values from the standard theory, given by Eq. (14), for the r^γ and r parameters. Under this assumption, the result in Eq. (12) can be converted to the j parameters as:

$$j_{\rm tot} = 0.046 \pm 0.034, \quad j_{\rm fb} = 0.807 \pm 0.042, \tag{17}$$

with the error correlation of -0.409. This result is to be compared with the standard-theory values from Eq. (14) of $j_{\rm tot} = 0.004$ and $j_{\rm fb} = 0.799$.

Similar measurements on the S-matrix parameters have been carried out by LEP experiments, by including their new data at energies beyond the Z^0 resonance [36]. The ALEPH group at LEP has obtained another constraint using $\mu^+\mu^-\gamma$ events, mainly accumulated around the Z^0 peak [37]. This measurement is sensitive to the reaction at c.m. energies below the peak where the Z^0 exchange is dominant. These measurements, including ours, are complementary to each other, since they are concerned with the reaction in qualitatively different energy regions.

D. Contact interaction

The sensitivity to the underlying physics can also be evaluated by introducing new interactions. Here we examine the hypothesis of contact interactions proposed by Eichten *et al.* [27]. In this model, new interactions are assumed to be described by direct couplings between helicity-conserving fermion currents.

It is convenient to use helicity amplitudes, when we consider only those interactions conserving the fermion helicity. The amplitudes for the muon-pair production can be written as

$$A_{ij}(s) = \alpha(s) q^e q^\mu + \alpha_Z g_i^e g_j^\mu \chi(s) \tag{18}$$

in the standard theory, where i and j denote the helicity (L or R) of the initial-state electron current and the final-state muon current, respectively. The parameters $\alpha(s)$ and α_Z are given previously. The parameters q^e and q^μ are the electric charges; both are -1 in this case. The chiral couplings to Z^0 are given by the effective couplings in Eq. (16) as:

$$g_L^\ell = v_\ell + a_\ell, \quad g_R^\ell = v_\ell - a_\ell, \tag{19}$$

for both $\ell = e$ and μ. The resonance function is given as

$$\chi(s) = \frac{s}{s - m_Z^2 + is\Gamma_Z/m_Z}, \tag{20}$$

using the s-dependent width.

The differential cross section is described as

$$\frac{d\sigma}{d\Omega} = \frac{1}{16s}\left\{(|A_{LL}|^2 + |A_{RR}|^2)(1+\cos\theta)^2 + (|A_{LR}|^2 + |A_{RL}|^2)(1-\cos\theta)^2\right\}. \tag{21}$$

Thus, the total cross section and the FB asymmetry are given as:

$$\begin{aligned} \sigma_{\rm TOT} &= \frac{\pi}{3s}\left(|A_{LL}|^2 + |A_{RR}|^2 + |A_{LR}|^2 + |A_{RL}|^2\right), \\ \sigma_{\rm FB} &= \frac{\pi}{4s}\left(|A_{LL}|^2 + |A_{RR}|^2 - |A_{LR}|^2 - |A_{RL}|^2\right), \end{aligned} \tag{22}$$

and $A_{\rm FB} = \sigma_{\rm FB}/\sigma_{\rm TOT}$.

The contact interactions of Eichten *et al.* can be introduced by adding the term,

$$A_{ij}^{\rm cont}(s) = \eta_{ij}\varepsilon s, \tag{23}$$

to Eq. (18), where ε is defined by the contact-interaction scale Λ as

$$\varepsilon = \pm\frac{1}{(\Lambda^\pm)^2}. \tag{24}$$

We can obtain the constraints on ε, by fitting Eq. (22) to the experimental result of Eq. (12). The results are shown in Table V for typical coupling cases. See elsewhere [27,38] for the definition of the couplings. The results are compared with those from a combined fit by

Kroha [38], including data from experiments at PEP and PETRA colliders and early VENUS data, and the recent results from the OPAL experiment at LEP based on their data up to 161 GeV [39]. In most cases, our results show the best sensitivity, *i.e.*, the smallest error for ε. The combined results, obtained from a weighted average, are also presented in Table V.

It should be noticed that the result by Kroha shows a relatively large deviation from the null contribution in the VV-coupling case. The significance is about two standard deviations. This result corresponds to the trend in the measurements at PETRA. The present measurement does not support such a large deviation.

The constraints on ε can be converted to lower limits on the contact-interaction scale Λ. The limits at the 95% confidence level (C.L.), obtained according to the definition given by Eq. (29) in Ref. [11], are presented in Table VI for the results from the present measurement and the combined results.

E. Neutral-scalar exchange

In the previous discussions, we considered only those interactions which conserve the helicity of the fermions. Such interactions necessarily lead to differential cross sections described in the form of Eq. (11). They are characterized by only two parameters, $\sigma_{\rm TOT}$ and $A_{\rm FB}$. Interactions which do not conserve the fermion helicity result in different angular distributions. One of the simplest examples for such interactions is the exchange of a heavy neutral-scalar (pseudoscalar) boson.

The muon-pair production via a neutral-scalar exchange leads to an isotropic distribution of the final-state muons. The differential cross section can be described as

$$\frac{d\sigma_{\rm S}}{d\Omega} = \frac{\sigma_{\rm S}}{4\pi} = \frac{s}{m_{\rm S}^2}\frac{\Gamma_{ee}\Gamma_{\mu\mu}}{(s-m_{\rm S}^2)^2 + (m_{\rm S}\Gamma_{\rm S})^2}, \tag{25}$$

where $m_{\rm S}$ and $\Gamma_{\rm S}$ are the mass and the total decay width of the scalar boson, respectively. The partial decay width to the $\ell^+\ell^-$ pair is written as $\Gamma_{\ell\ell}$.

The cross section to be observed is the sum of Eq. (11) and Eq. (25), because of the absence of the interference. We can obtain the constraint on the scalar-exchange cross section ($\sigma_{\rm S}$), by fitting the sum to the measured differential cross section in Table IV. Using the standard-theory predictions from ALIBABA, $\sigma_{\rm TOT}^{\rm EB} = 30.74$ pb and $A_{\rm FB}^{\rm EB} = -0.338$, we obtain a constraint as

$$\sigma_{\rm S} = -0.60 \pm 0.48 \text{ pb}. \tag{26}$$

This result can be converted to an upper limit of 0.63 pb at the 95% C.L., according to the definition used for the limits on the contact interaction. If we assume that the c.m. energy is out of the resonance region, this cross-section limit can be converted to the limits on the partial decay widths as $\Gamma_{ee}\Gamma_{\mu\mu} < (22 \text{ MeV})^2$ for $m_{\rm S} = 70$ GeV/c^2, and $\Gamma_{ee}\Gamma_{\mu\mu} < (48 \text{ MeV})^2$ for $m_{\rm S} = 80$ GeV/c^2.

Possible contributions of neutral-scalar bosons, with the mass within or around the energy coverage, were investigated in our previous studies, for the reactions $e^+e^- \to$ hadrons [40] and $e^+e^- \to e^+e^-$ and $\gamma\gamma$ [41]. These studies lead to negative results and set constraints on the scalar-boson couplings. A constraint for heavier cases has been obtained from a study

of Bhabha scattering [11]. Studies for the scalar bosons within our energy coverage were also carried out by other groups at TRISTAN [42,43]. The study by the TOPAZ group [43] included the reaction $e^+e^- \to \mu^+\mu^-$. The present result adds supplementary information to the results obtained thus far.

VI. CONCLUSIONS

The reaction $e^+e^- \to \mu^+\mu^-$ was measured at $\sqrt{s} = 57.77$ GeV using the VENUS detector at TRISTAN. A total of 4484 events were identified from 289.6 ± 2.6 pb^{-1} data, within the angular acceptance of $|\cos\theta| \leq 0.75$.

The production cross section was measured according to the definition of signal events that $|\cos\theta_{\mu^+,\mu^-}| \leq 0.75$, $p_{\mu^+,\mu^-} \geq E_{\rm beam}/2$ and $\theta_{\rm acol} \leq 10°$. The measurement result is independent of any theories and models describing the reaction, since corrections depending on them, such as those for photon-radiation effects and angular extrapolations, are not applied.

The cross section measured in bins of the production angle is presented in Table I. The error correlation between the bins was treated in the form of an error matrix. The correlation matrix for the error of the result in Table I is presented in Table II. The total cross section and the forward-backward (FB) asymmetry for the signal events were obtained as $\sigma^{\rm signal} = 17.69 \pm 0.35$ pb and $A_{\rm FB}^{\rm signal} = -0.254 \pm 0.017$, respectively.

The model-independent result was found to be consistent with predictions from computer programs based on the standard electroweak theory (ALIBABA, ZFITTER and KORALZ). The consistency was confirmed not only in the global behavior, $\sigma^{\rm signal}$ and $A_{\rm FB}^{\rm signal}$, but also in the direct comparison of the binned cross section.

The trend in the measurements at lower energies, that the total cross section is smaller than the standard-theory prediction while the FB asymmetry is in good agreement, remains in the present result. However, the observed discrepancy in the total cross section is only 1.1-times the measurement error. It should be reminded that the discrepancy at lower energies can be recognized only in the combined results of many experiments. There may be unaccounted correlations between the measurements. Thus, these observations are not enough to emphasize the presence of the discrepancy.

The binned cross section was converted to the differential cross section in the effective-Born (EB) scheme, using the estimate of the photon-radiation effects from ALIBABA. From a fit to the result, the total cross section and the FB asymmetry extrapolated to the full solid angle were evaluated as $\sigma_{\rm TOT}^{\rm EB} = 30.05 \pm 0.59$ pb and $A_{\rm FB}^{\rm EB} = -0.350 \pm 0.017$, respectively, under the assumption that the reaction originates from helicity-conserving interactions only.

The obtained EB cross section was used to set constraints on possible extensions of the standard theory. The interference parameters in the simplest S-matrix parametrization were determined as $j_{\rm tot} = 0.046 \pm 0.034$ and $j_{\rm fb} = 0.807 \pm 0.042$, assuming the standard-theory values for the direct contributions of the photon and Z^0 exchanges.

Constraints were also evaluated for the contact interactions introduced by Eichten *et al.* The lower limit on the energy scale of the interaction was obtained to be $2 - 6$ TeV at the 95% C.L., depending on the assumed coupling. The present measurement shows the best sensitivity among measurements carried out so far, for most of the typical combinations of

the coupling. Combined constraints were also evaluated. The results are presented in Tables V and VI.

Possible contributions of heavy neutral-scalar exchanges were examined using the differential EB cross section. The contribution was found to be smaller than 0.63 pb at the 95% C.L. This limit corresponds to the constraints on the partial decay widths, as $\Gamma_{ee}\Gamma_{\mu\mu} < (22\ {\rm MeV})^2$ for the scalar-boson mass of 70 GeV/c^2, and $\Gamma_{ee}\Gamma_{\mu\mu} < (48\ {\rm MeV})^2$ for 80 GeV/c^2.

ACKNOWLEDGMENTS

We wish to thank the TRISTAN machine group for their patient efforts regarding the accelerator operation that continued for many years. We gratefully acknowledge the outstanding contributions of the technical staff at KEK and the collaborating institutes who participated in the construction and operation of the VENUS detector. The data acquisition and analyses were made possible with continuous support by people from the online group and the computer center of KEK. We would like to thank W. Beenakker for his advice concerning the use of ALIBABA and discussions about theoretical errors. We thank B. Pietrzyk, who gave us the ALEPH version of BABAMC with his useful comments. We also thank M. Caffo and H. Czyż for discussions about theoretical errors for Bhabha scattering.

REFERENCES

[1] JADE Collaboration, W. Bartel *et al.*, Phys. Lett. **108B**, 140 (1982); TASSO Collaboration, R. Brandelik *et al.*, *ibid.* **110B**, 173 (1982); Mark J Collaboration, B. Adeva *et al.*, Phys. Rev. Lett. **48**, 1701 (1982); CELLO Collaboration, H.J. Behrend *et al.*, Z. Phys. C **14**, 283 (1982).

[2] HRS Collaboration, D. Bender *et al.*, Phys. Rev. D **30**, 515 (1984); M. Derrick *et al.*, *ibid.* **31**, 2352 (1985); MAC Collaboration, E. Fernandez *et al.*, Phys. Rev. Lett. **50**, 1238 (1983); W.W. Ash *et al.*, *ibid.* **55**, 1831 (1985); Mark II Collaboration, M.E. Levi *et al.*, *ibid.* **51**, 1941 (1983).

[3] CELLO Collaboration, H.J. Behrend *et al.*, Phys. Lett. B **191**, 209 (1987); JADE Collaboration, W. Bartel *et al.*, Z. Phys. C **26**, 507 (1985); **30**, 371 (1986); S. Hegner *et al.*, *ibid.* **46**, 547 (1990); Mark J Collaboration, B. Adeva *et al.*, Phys. Rev. Lett. **55**, 665 (1985); Phys. Rev. D **38**, 2665 (1988); PLUTO Collaboration, Ch. Berger *et al.*, Z. Phys. C **21**, 53 (1983); **27**, 341 (1985); TASSO Collaboration, M. Althoff *et al.*, *ibid.* **22**, 13 (1984); W. Braunschweig *et al.*, *ibid.* **40**, 163 (1988).

[4] VENUS Collaboration, K. Abe *et al.*, Z. Phys. C **48**, 13 (1990); Phys. Lett. B **246**, 297 (1990).

[5] AMY Collaboration, A. Bacala *et al.*, Phys. Lett. B **218**, 112 (1989); C. Velissaris *et al.*, *ibid.* **331**, 227 (1994); TOPAZ Collaboration, I. Adachi *et al.*, *ibid.* **208**, 319 (1988); B. Howell *et al.*, *ibid.* **291**, 206 (1992).

[6] For the most recent results see: ALEPH Collaboration, D. Buskulic *et al.*, Z. Phys. C **62**, 539 (1994); DELPHI Collaboration, P. Abreu *et al.*, Nucl. Phys. **B418**, 403 (1994); L3 Collaboration, M. Acciarri *et al.*, Z. Phys. C **62**, 551 (1994); OPAL Collaboration, R. Akers *et al.*, *ibid.* **61**, 19 (1994); SLD Collaboration, K. Abe *et al.*, Phys. Rev. Lett. **79**, 804 (1997).

[7] ALEPH Collaboration, D. Buskulic *et al.*, Phys. Lett. B **378**, 373 (1996); L3 Collaboration, M. Acciarri *et al.*, *ibid.* **370**, 195 (1996); *ibid.* **407**, 361 (1997); OPAL Collaboration, G. Alexander *et al.*, *ibid.* **376**, 232 (1996); K. Ackerstaff *et al.*, *ibid.* **391**, 221 (1997).

[8] S. Weinberg, Phys. Rev. Lett. **19**, 1264 (1967); A. Salam, in *Elementary Particle Theory: Relativistic Groups and Analyticity (Nobel Symposium No. 8)*, edited by N. Svartholm (Almqvist and Wiksells, Stockholm, 1968), p. 267.

[9] U. Amaldi *et al.*, Phys. Rev. D **36**, 1385 (1987).

[10] K. Hagiwara, R. Najima, M. Sakuda, and N. Terunuma, Phys. Rev. D **41**, 815 (1990).

[11] VENUS Collaboration, T. Arima *et al.*, Phys. Rev. D **55**, 19 (1997).

[12] R. Arai *et al.*, Nucl. Instrum. Methods Phys. Res. A **254**, 317 (1987).

[13] TRISTAN Project Group, *TRISTAN Electron-positron Colliding Beam Project*, KEK Report 86-14 (1987).

[14] R. Arai *et al.*, Nucl. Instrum. Methods Phys. Res. A **217**, 181 (1983); S. Odaka, KEK Preprint 88-5 (1988), unpublished.

[15] Y. Hemmi *et al.*, Jpn. J. Appl. Phys. **26**, 982 (1987).

[16] K. Ogawa *et al.*, Nucl. Instrum. Methods Phys. Res. A **243**, 58 (1986); T. Sumiyoshi *et al.*, *ibid.* **271**, 432 (1988).

[17] Y. Asano *et al.*, Nucl. Instrum. Methods Phys. Res. A **254**, 35 (1987); *ibid.* **259**, 430 (1987).

[18] T. Ohsugi *et al.*, Nucl. Instrum. Methods Phys. Res. A **269**, 522 (1988).

[19] Y. Arai and S. Uehara, Nucl. Instrum. Methods Phys. Res. A **301**, 497 (1991).

[20] W. Beenakker, F.A. Berends, and S.C. van der Marck, Nucl. Phys. **B349**, 323 (1991).

[21] A part of the program, QEDPS-Bhabha, being developed by K. Tobimatsu.

[22] H. Burkhardt, F. Jegerlehner, G. Penso, and C. Verzegnassi, Z. Phys. C **43**, 497 (1989).

[23] K. Tobimatsu and Y. Shimizu, Prog. Theor. Phys. **74**, 567 (1985); **76**, 334 (1986); **75**, 905 (1986); S. Kuroda *et al.*, Comput. Phys. Commun. **48**, 335 (1988).

[24] M. Böhm, A. Denner, and W. Hollik, Nucl. Phys. **B304**, 687 (1988); F.A. Berends, R. Kleiss, and W. Hollik, *ibid.* **B304**, 712 (1988). We used the program that has been modified by the ALEPH group so as to implement the vacuum-polarization formula in Ref. [22].

[25] S. Jadach, E. Richter-Wąs, B.F.L. Ward, and Z. Wąs, Comput. Phys. Commun. **70**, 305 (1992).

[26] M. Caffo, H. Czyż, and E. Remiddi, Phys. Lett. B **327**, 369 (1994).

[27] E.J. Eichten, K.D. Lane, and M.E. Peskin, Phys. Rev. Lett. **50**, 811 (1983).

[28] J. Fujimoto *et al.*, Prog. Theor. Phys. Suppl. **100**, 1 (1990); M. Igarashi *et al.*, Nucl. Phys. **263**, 347 (1986).

[29] T. Sjöstrand and M. Bengtsson, Comput. Phys. Commun. **46**, 43 (1987); **39**, 347 (1986).

[30] S. Jadach, B.F.L. Ward, and Z. Wąs, Comput. Phys. Commun. **79**, 503 (1994).

[31] VENUS Collaboration, H. Hanai *et al.*, Phys. Lett. B **403**, 155 (1997).

[32] F.A. Berends, P.H. Daverveldt, and R. Kleiss, Comput. Phys. Commun. **40**, 285 (1986).

[33] D. Bardin *et al.*, CERN-TH. 6443/92 (1992).

[34] A. Borrelli, M. Consoli, L. Maiani, and R. Sisto, Nucl. Phys. **B333**, 357 (1990); L. Leike, T. Riemann, and J. Rose, Phys. Lett. B **273**, 513 (1991).

[35] M. Consoli and W. Hollik, in *Z Physics at LEP I*, edited by G. Altarelli *et al.*, CERN 89-08 (1989), Vol. 1, p. 7.

[36] L3 Collaboration, M. Acciarri *et al.*, Phys. Lett. B **370**, 195 (1996); *ibid.* **407**, 361 (1997); OPAL Collaboration, G. Alexander *et al.*, *ibid.* **376**, 232 (1996); K. Ackerstaff *et al.*, *ibid.* **391**, 221 (1997).

[37] ALEPH Collaboration, R. Barate *et al.*, Phys. Lett. B **399**, 329 (1997).

[38] H. Kroha, Phys. Rev. D **46**, 58 (1992).

[39] OPAL Collaboration, K. Ackerstaff *et al.*, Phys. Lett. B **391**, 221 (1997).

[40] VENUS Collaboration, S. Odaka *et al.*, J. Phys. Soc. Jpn. **58**, 3037 (1989).

[41] VENUS Collaboration, K. Abe *et al.*, Phys. Lett. B **302**, 119 (1993).

[42] AMY Collaboration, K.L. Sterner *et al.*, Phys. Lett. B **303**, 385 (1993).

[43] TOPAZ Collaboration, K. Abe *et al.*, Phys. Lett. B **304**, 373 (1993).

TABLES

TABLE I. Primary model-independent result of the present measurement. The number of muon-pair candidates is subdivided into angular bins (N_i), according to the cosine of the production angle of μ^- ($\cos\theta$). The number of events is converted to the cross section for the signal events ($\sigma_i^{\rm signal}$), using the estimated background contamination ($N_i^{\rm bkg}$) and detection efficiency (ε_i), together with the integrated luminosity determined from small-angle Bhabha scattering. The error of $\sigma_i^{\rm signal}$ includes the error from the data statistics, as well as those from the corrections and the luminosity determination. The correlation matrix for the error is shown in Table II. The prediction of the standard electroweak theory, obtained from ALIBABA, is presented in the last column.

Bin	$\cos\theta$	N_i	$N_i^{\rm bkg}$	$1-\varepsilon_i$ (%)	$\sigma_i^{\rm signal}$ (pb)	ALIBABA (pb)
1	$-0.75 \sim -0.50$	1187	11.7 ± 2.0	13.5 ± 1.5	4.69 ± 0.16	4.77
2	$-0.50 \sim -0.25$	915	8.8 ± 2.4	13.6 ± 1.6	3.62 ± 0.14	3.72
3	$-0.25 \sim 0.0$	712	7.5 ± 1.6	12.6 ± 1.9	2.78 ± 0.12	2.87
4	$0.0 \sim 0.25$	602	7.6 ± 1.5	16.7 ± 2.4	2.46 ± 0.12	2.34
5	$0.25 \sim 0.50$	524	6.1 ± 1.4	12.9 ± 2.1	2.05 ± 0.10	2.13
6	$0.50 \sim 0.75$	544	14.0 ± 2.1	11.8 ± 1.9	2.08 ± 0.10	2.23

TABLE II. Correlation matrix for the error of the signal cross section ($\sigma_i^{\rm signal}$) presented in Table I. This matrix is also relevant to the error of the differential cross section ($d\sigma_i^{\rm EB}/d\Omega$) in Table IV.

Bin	1	2	3	4	5	6
1	1	0.080	0.076	0.052	0.056	0.060
2		1	0.074	0.041	0.050	0.050
3			1	0.005	0.029	0.035
4				1	0.060	0.055
5					1	0.046
6						1

TABLE III. Summary of the total cross section and the forward-backward asymmetry, within the angular acceptance of $|\cos\theta| \leq 0.75$. The measurement results, obtained from the sum of the binned cross sections, are compared with the predictions from computer programs based on the standard electroweak theory (ALIBABA, ZFITTER and KORALZ). The comparison is made for the quantities in the signal definition of the present measurement, as well as those in the ZFITTER-like definition (ZF) and in the effective-Born scheme (EB). See the text for the definitions. The measurement results are converted to the ZF and EB quantities, using correction factors given by ALIBABA. The statistical error of the KORALZ results is smaller than 0.02 pb.

	Measurement	ALIBABA	ZFITTER	KORALZ
$\sigma^{\rm signal}$ (pb)	17.69 ± 0.35	18.07		18.08
$A_{\rm FB}^{\rm signal}$	-0.254 ± 0.017	-0.258		
$\sigma^{\rm ZF}$ (pb)	17.86 ± 0.35	18.25	18.10	18.26
$A_{\rm FB}^{\rm ZF}$	-0.256 ± 0.017	-0.260	-0.262	
$\sigma^{\rm EB}(0.75)$ (pb)	20.11 ± 0.39	20.54	20.54	20.56
$A_{\rm FB}^{\rm EB}(0.75)$	-0.280 ± 0.017	-0.284	-0.284	

TABLE IV. Differential cross section in the effective-Born scheme. The binned cross section ($\sigma_i^{\rm signal}$) in Table I was converted to the differential cross section ($d\sigma_i^{\rm EB}/d\Omega$) at the center of the bins ($\cos\theta_i$), using the photon-radiation (QED) correction ($\delta_i^{\rm rad}$) and the correction for the binning effect ($\delta_i^{\rm bin}$), estimated by using ALIBABA. The error correlation shown in Table II is also relevant to this result.

Bin	$\cos\theta_i$	$\delta_i^{\rm rad}$	$\delta_i^{\rm bin}$	$d\sigma_i^{\rm EB}/d\Omega$ (pb/str)
1	-0.625	-0.155	0.0027	3.52 ± 0.12
2	-0.375	-0.129	0.0035	2.64 ± 0.10
3	-0.125	-0.121	0.0046	2.01 ± 0.09
4	0.125	-0.107	0.0058	1.75 ± 0.09
5	0.375	-0.085	0.0065	1.42 ± 0.07
6	0.625	-0.071	0.0063	1.41 ± 0.07

TABLE V. Constraints on the contact-interaction parameter ε. The best fit values are shown with one standard-deviation errors. The constraints are evaluated for typical combinations of the initial-state and final-state helicities. The results from the present measurement are presented, together with those from a combined fit by Kroha [38], including previous measurements at PEP, PETRA and TRISTAN, and with recent results from the OPAL experiment at LEP [39]. The combined results, obtained from a weighted average, are also presented.

	ε (TeV^{-2})				
	LL	RR	LR	VV	AA
This expt.	-0.106 ± 0.082	-0.097 ± 0.074	-0.057 ± 0.069	-0.031 ± 0.023	-0.009 ± 0.029
Kroha	-0.155 ± 0.095	-0.148 ± 0.093	-0.072 ± 0.095	-0.074 ± 0.038	-0.018 ± 0.030
OPAL	$0.051^{+0.073}_{-0.074}$	$0.054^{+0.079}_{-0.082}$	$0.103^{+0.078}_{-0.088}$	$0.034^{+0.030}_{-0.030}$	$-0.006^{+0.036}_{-0.035}$
Combined	-0.053 ± 0.048	-0.060 ± 0.047	-0.017 ± 0.047	-0.020 ± 0.016	-0.011 ± 0.018

TABLE VI. Lower limits of the contact-interaction scale Λ at the 95% C.L., corresponding to the constraints on ε in Table V. The limits were evaluated for the results from the present measurement and for the combined results.

	95%-C.L. limit of Λ (TeV)									
	LL		RR		LR		VV		AA	
	+	−	+	−	+	−	+	−	+	−
This expt.	3.1	2.0	3.2	2.1	3.1	2.4	5.9	3.8	4.4	4.0
Combined	3.9	2.7	4.0	2.6	3.5	3.1	6.9	4.6	5.9	4.8

FIGURES

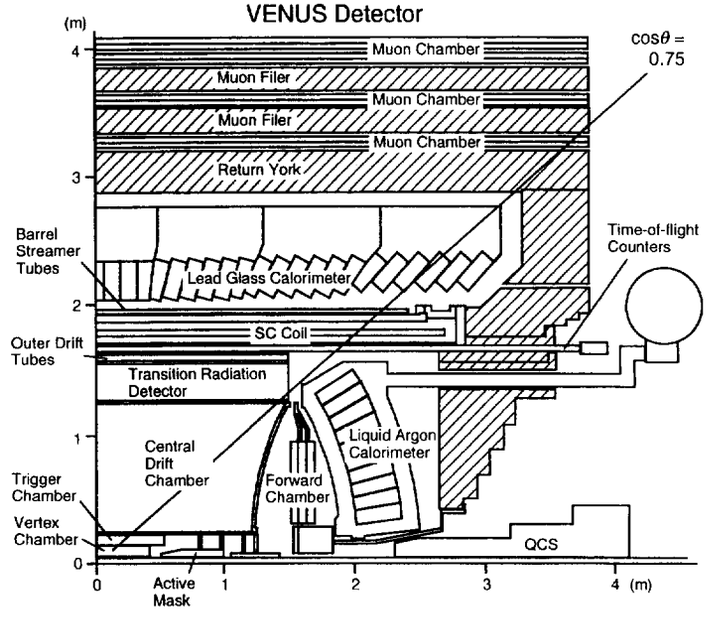

FIG. 1. Quadrant cross section of the upgraded VENUS detector. The edge of the angular acceptance is indicated with a line.

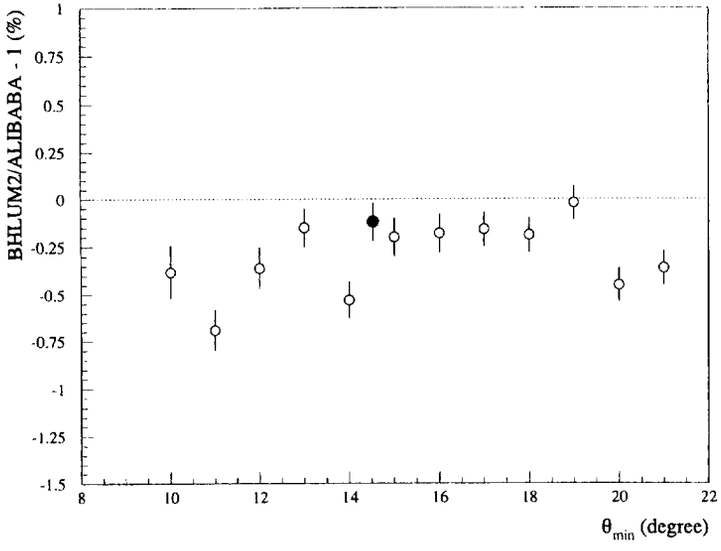

FIG. 2. Comparison between the results of **BHLUM2** and **ALIBABA** for the small-angle Bhabha scattering. The difference in the total cross section is plotted as a function of the lower angle-cut ($\theta_{\rm min}$) in the signal definition. The filled circle corresponds to our definition.

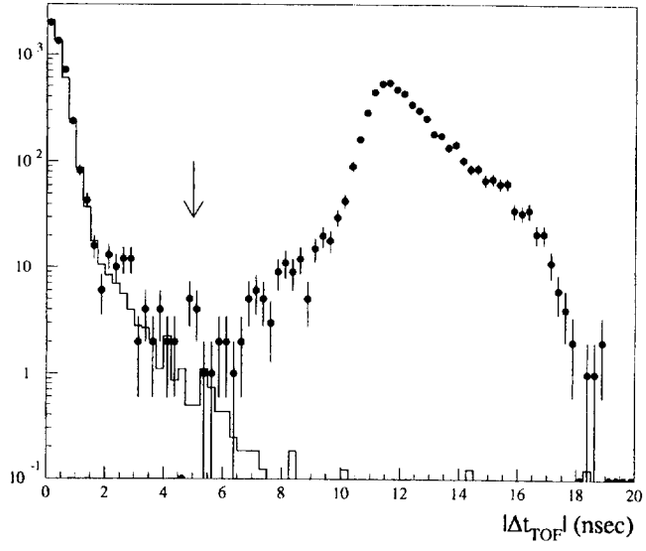

FIG. 3. Distribution of the flight-time difference between the two tracks, $|\Delta t_{\rm TOF}|$. The $|\Delta t_{\rm TOF}|$ cut was excluded to make the plot. We can see a good separation between the muon-pair events (small $|\Delta t_{\rm TOF}|$) and cosmic-ray events ($|\Delta t_{\rm TOF}| \gtrsim 10$ nsec). The arrow indicates the cut in the event selection. The histogram shows the distribution for Bhabha-scattering events normalized to the muon-pair candidates.

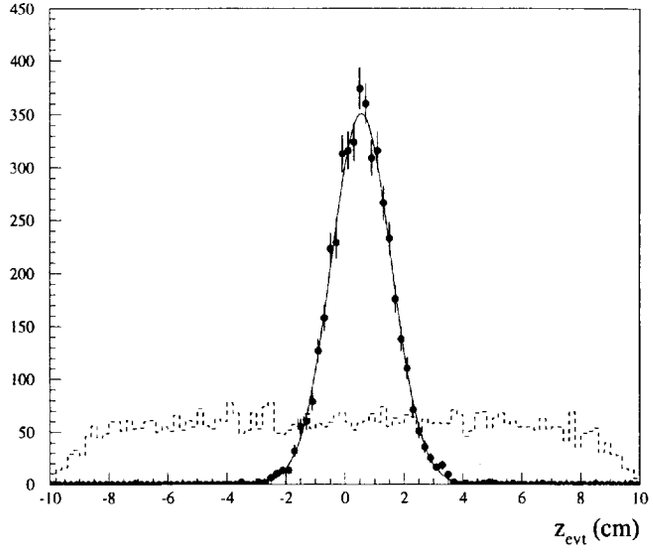

FIG. 4. Distribution of the event vertex along the beam direction for the muon-pair candidates. The curve shows the fit by a Gaussian distribution, having a standard deviation of 1.0 cm. The distribution shows the profile of the interaction point. The measurement resolution is better than the observed spread. The dashed histogram shows the distribution for cosmic-ray events, collected with the condition, $|\Delta t_{\rm TOF}| > 8$ nsec.

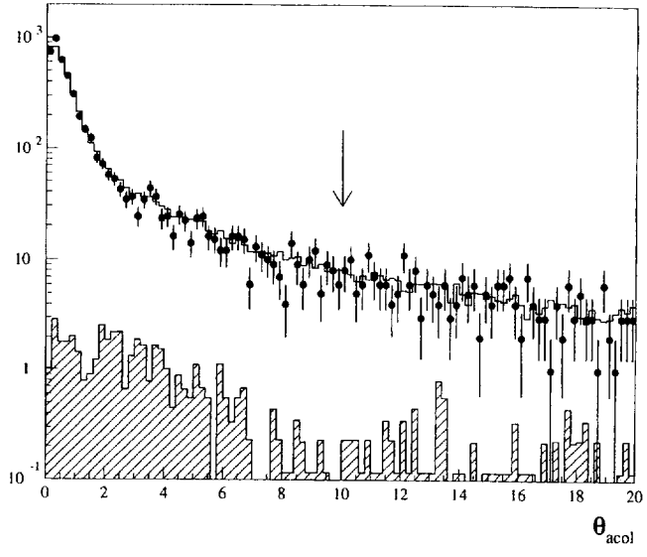

FIG. 5. Distribution of the acollinearity angle between the two tracks. The simulation (histogram) is compared with the candidate events (plot). The requirement on the acollinearity angle is loosened, in order to look at the behavior around the cut, indicated with the arrow. The simulation includes the contribution of background, tau-pair and $e^+e^-\mu^+\mu^-$ events, separately shown with the hatched histogram. The simulation of the muon-pair events, based on the FS program, is normalized to the total yield of the candidate events.

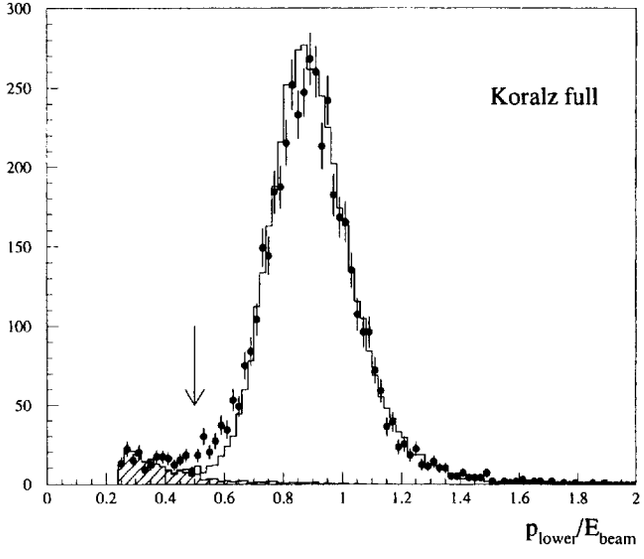

FIG. 6. Momentum distribution of the lower-momentum tracks in the muon-pair candidates. The momentum cut is lowered to $E_{\rm beam}/4$, in order to look at the behavior around and below the cut in the standard selection indicated with the arrow. The definitions of the histograms are the same as Fig. 5, except that KORALZ and a full detector simulator are used for the muon-pair events, intending to reproduce the non-Gaussian behavior in the data distribution.

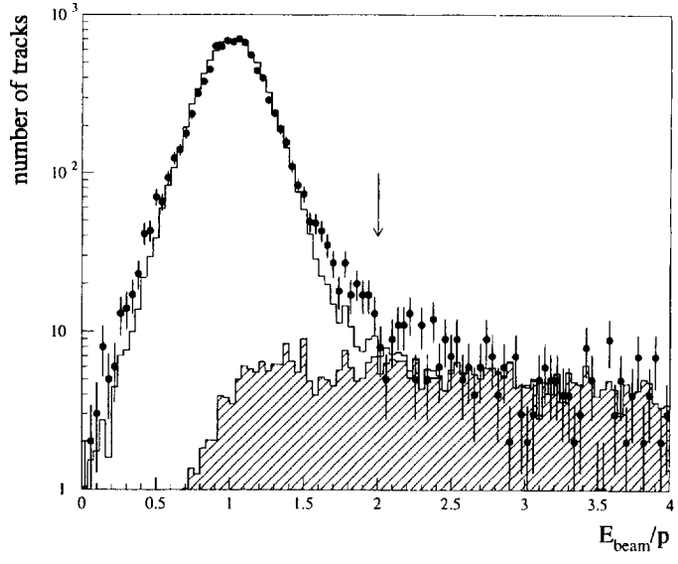

FIG. 7. $E_{\rm beam}/p$ distribution for the same event sample as used in Fig. 6. The two tracks in the events are used. The simulations (histograms) are also the same as Fig. 6. The arrow indicates the cut in the standard selection.

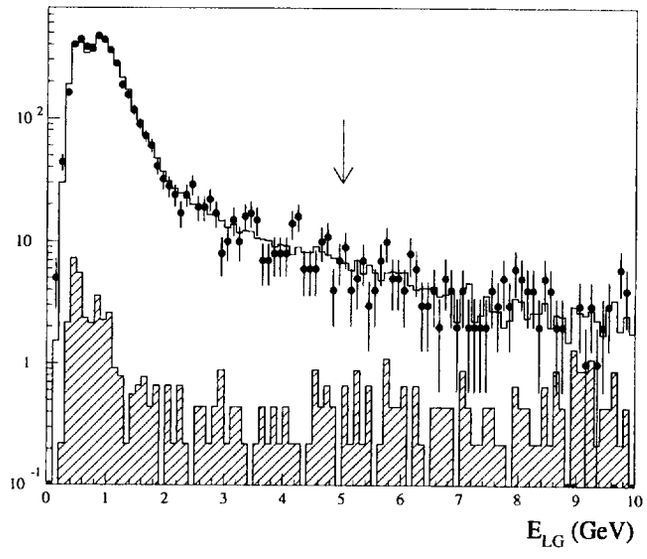

FIG. 8. LG-energy spectrum for the candidate events. The LG-energy cut is loosened to show the spectrum around the standard cut indicated with the arrow. The definitions of the histograms are the same as Fig. 5.

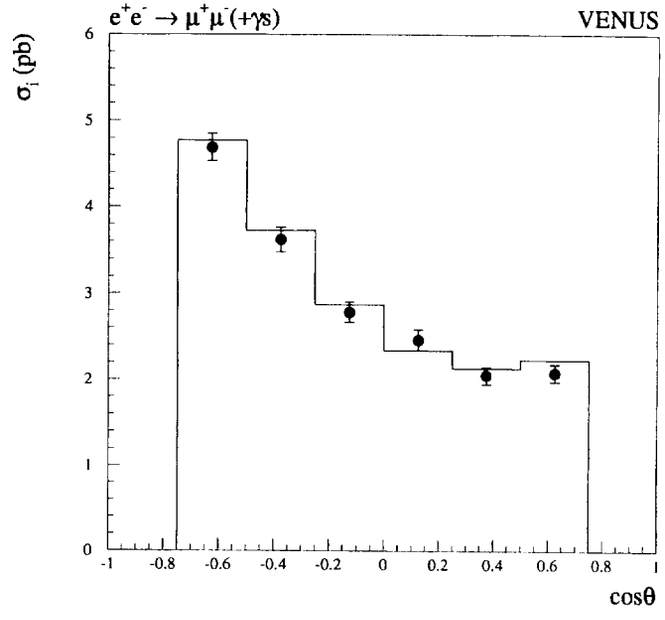

FIG. 9. Measured model-independent cross section for the signal events. The result is binned according to the cosine of the production angle of μ^-. The histogram shows the prediction from ALIBABA.

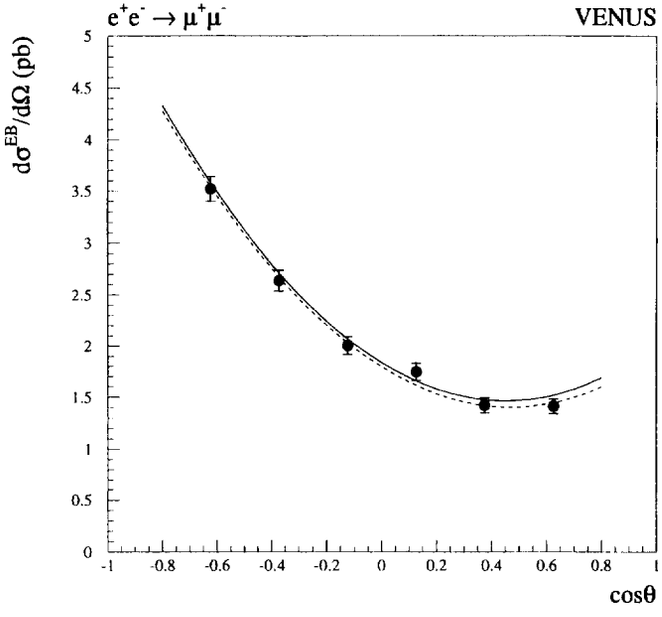

FIG. 10. Measured differential cross section in the effective-Born scheme. The solid curve represents the prediction of the standard electroweak theory, given by ALIBABA. The dashed curve shows the best fit of the formula defined in the text.